



---

Final Degree Project

---

Chemistry Degree

# Synthesis and characterization of biocompatible shape-memory polyurethanes

Author:

**Ane Martín Ayerdi**

Director:

**Dr. Antonio Veloso Fernández**

Co-Director:

**Dra. Leyre Pérez Álvarez**



## FINAL DEGREE PROJECT

### CHEMISTRY DEGREE

# SYNTHESIS AND CHARACTERIZATION OF BIOCOMPATIBLE SHAPE-MEMORY POLYURETHANES

REPORT PRESENTED BY ANE MARTÍN AYERDI

**REGISTRATION AND DEFENSE DATE:** February 2021/March 2021

**DIRECTOR:** Antonio Veloso Fernández

**CO-DIRECTOR:** Leyre Pérez Álvarez

**DEPARTMENT:** Macromolecular Physical – Chemistry

## INDEX

Page

<b>1. <u>INTRODUCTION</u></b> .....	<b>1</b>
<b>2. <u>OBJETIVES</u></b> .....	<b>17</b>
<b>3. <u>DEVELOPMENT</u></b> .....	<b>18</b>
<b>3.1. REAGENTS</b> .....	<b>18</b>
<b>3.2. SYNTHESIS</b> .....	<b>18</b>
<b>3.3 CHARACTERIZATION</b> .....	<b>22</b>
<b>3.3.1 Attenuated total reflection-Fourier transform infrared spectroscopy ..</b>	<b>22</b>
<b>3.3.2 Thermogravimetric analysis</b> .....	<b>23</b>
<b>3.3.3 Differential scanning calorimetry</b> .....	<b>24</b>
<b>3.3.4 Dynamic mechanical analysis</b> .....	<b>25</b>
<b>3.3.5 Thermomechanical analysis</b> .....	<b>27</b>
<b>3.3.6 Cytotoxic analysis</b> .....	<b>28</b>
<b>4. <u>RESULTS AND DISCUSSION</u></b> .....	<b>29</b>
<b>4.1 SAMPLE CHARACTERIZATION AT NCO/OH= 1 RATIO</b> .....	<b>29</b>
<b>4.2 SAMPLE CHARACTERIZATION AT NCO/OH= 1.05 AND 1.1 RATIOS</b> .....	<b>36</b>
<b>4.3 CYTOTOXIC ANALYSIS</b> .....	<b>39</b>
<b>5. <u>CONCLUSIONS</u></b> .....	<b>40</b>
<b>6. <u>FUTURE WORK</u></b> .....	<b>41</b>
<b>7. <u>ACKNOWLEDGMENTS</u></b> .....	<b>42</b>
<b>8. <u>REFERENCES</u></b> .....	<b>42</b>
<b>9. <u>ATTACHMENTS</u></b> .....	<b>47</b>
<b>9.1 ACRONYMS</b> .....	<b>47</b>
<b>9.2 TABLES</b> .....	<b>50</b>

## 1. INTRODUCTION

Currently there is a great demand and interest in *stimulus-responsive materials* (SRMs) since they provide a very attractive insight into materials science. Among them, one group is known as *shape-memory materials* (SMMs) which are able to change their shape in presence of a stimulus. That effect is known as *shape-memory effect* (SME), where the material is able to deform and fix into a temporary stage applying an external stimulus, and when the stimulus is removed their original shape is recovered.<sup>1</sup> Some of the used stimuli used are: heat (thermo-responsive material), electrical current/voltage (electro-responsive material), magnetic field (magneto-responsive material), pH-change/solvent (chemo-responsive material) and light (photo-responsive material).<sup>2,3</sup> There are a number of types of SMMs which have been developed so far, such as alloys (SMAs), polymers (SMPs), hybrids (SMHs) and ceramics (SMCs).

SMAs fall into two categories, one is thermo-responsive and the other is magneto-responsive or, ferromagnetic materials, which are divided in three major types named as Cu-based (mainly CuAlNi and CuZnAl), NiTi- and Fe-based (FeMnSi, FeNiC and FeNiCoTi). SMHs allow to mix different matrices (organic, inorganic and metals) and inclusions to improve materials properties. Inside SMCs zirconia (ZrO<sub>2</sub>)-based ceramics can be found. Among different types, from now on, our attention will be focus on SMPs.<sup>1</sup>

SMPs increased attention due to their scientific and technological significance. They offer deformation to highest degree and widest scope of varying mechanical properties compared to SMAs or SMCs. Even more, polymers offer extra advantages owing to the fact that they may be biocompatible, non-toxic, biodegradable and can be made from bio-renewable resources.<sup>2</sup>

SME is performed in *one-way* or *two-way methods* (Figure 1). At a first stage, *programming*, both methods work in the same way, by means of a stimulus (stimulus on) the material is programmed to change from A shape to B shape. At that point, one-way SME method is over as the objective is to deform and fix in that new form. However, the two-way method continues in the second stage *recovery*, that is, removing the

stimulus (stimulus off) the polymer "remembers" its original shape and is able to recover the previous got A form.<sup>4</sup> The process explained is called *dual shape-memory effect* (DSME) since the polymer changes from A to B form, yet, this effect can be performed to get triple or multiple SME.

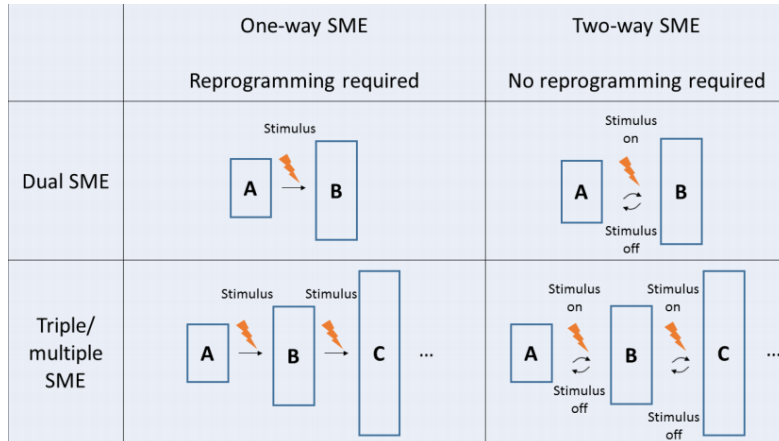


**Figure 1.** One-way and two-way SME scheme for dual (A-B shapes) and triple/multiple (A-B-C... shapes) SME mechanisms.<sup>4</sup>

The *triple shape-memory effect* (TSME) has the ability of memorizing two temporary shapes and sequentially recover their original shapes by heating, using a thermo-responsive material. In *Figure 2* we can see that TSME mechanism is related with dots and curled up strings. Dots are the segment with higher transition temperature ( $T_{Trans}$ ) while curled up stripes is the segment with lower  $T_{Trans}$ . Since two different transition temperatures are going to be used, higher transition temperature will be called as  $T_{Trans I}$  while lower transition temperature as  $T_{Trans II}$ . Primary the material has to be synthesised for giving the initial A shape. Then, in the seconds step the polymer is heated above a higher order temperature ( $T_{high}$ ), which is higher than the two transition temperatures ( $T_{Trans I}$  and  $T_{Trans II}$ ). During next steps, temperature will be decreased below each  $T_{trans}$ . *Figure 2* shows as colour change from red to blue when the  $T < T_{Trans}$ , while a stress in applied for giving the new shapes. In the third step, temperature is dropped below  $T_{Trans I}$  getting a colour change in dots, obtaining the new B shape which is slightly wider than A shape. Then in the fourth step, the temperature will keep on

decreasing below  $T_{Trans II}$ , turning out to see a colour change in *Figure 2* of curled up strings. After this, the polymer has changed into its new C shape which is wider and longer than previous shapes. Once the new two shapes have been achieved, the process will continue in order to recover the initial A shape. To obtain that, the polymer will be reheated above each  $T_{Trans}$  but without stress. In the fourth stage it is seen that curled up strings colour is red again. That happens because the temperature is higher than  $T_{Trans II}$ , allowing to the polymer to get the same shape that had in the third step. Finally in the fifth stage, dots have also recovered the red colour that had at the beginning, in other words, the temperature is higher than  $T_{Trans I}$ . Due to that, the polymer has recovered the initial A shape that had at the beginning.<sup>5</sup>

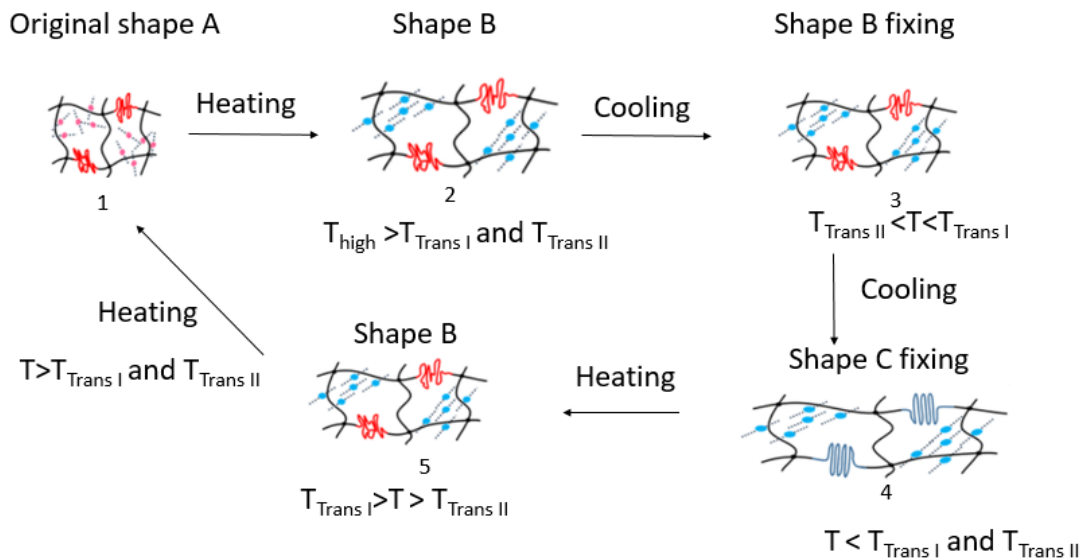


**Figure 2.** TSME mechanism, colour change of dots and curled up strings from red to blue representing shape change below  $T_{Trans}$  and from blue to red above  $T_{Trans}$ .<sup>6</sup> (Edited figure)

In order to verify the DSME performed in this work (*Figure 3*), heat has been used as stimulus. First, the polymer is synthesised receiving its initial shape, afterwards, programming step starts heating the polymer above  $T_{Trans}$ . Above this temperature, the structure of the polymer changes from stiff to plastic, allowing to give the shape wanted applying stress. Afterwards, the polymer is cooled below  $T_{Trans}$  freezing into its new

shape. The cycle finishes with recovery step, reheating above  $T_{Trans}$  and removing the stress recovering the initial shape.<sup>3,7</sup>

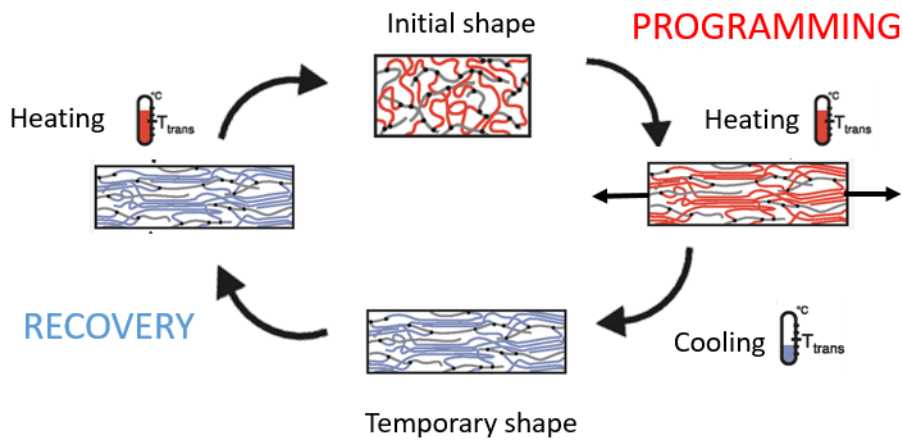


**Figure 3.** Dual shape-memory effect scheme, showing in red programming step and in blue recovery steps.<sup>2</sup> (Edited Figure)

Transition temperature can be related to any process that could happen while the sample is heated such as crystallisation ( $T_c$ ), fusion ( $T_m$ ) or glass transition temperature also known as vitreous transition state ( $T_g$ ). Among all of them, in this case is related to  $T_g$ . Above this temperature the stiff polymer becomes glassy or rubbery earning more ability to move the chain.<sup>4,5</sup>

Inside polymeric compounds two big groups can be found, on one hand those belonging to natural origin like starch, cellulose or silk and on the other hand, synthetic such as nylon, polyethylene, polystyrene and so on.<sup>8</sup> However, not all polymers can perform previously mentioned SME, since that effect depends on structure and morphology they have. Owing to that, the polymer chosen has been polyurethane (PU).

PU contains urethane group as monomer (Figure 4), synthesised from the polycondensation between an isocyanate ( $-NCO$ ) and hydroxyl ( $-OH$ ) groups. There were introduced in 1937 thanks to Professor Dr Otto Bayer through a reaction between diisocyanate and polyester diol.<sup>9</sup>



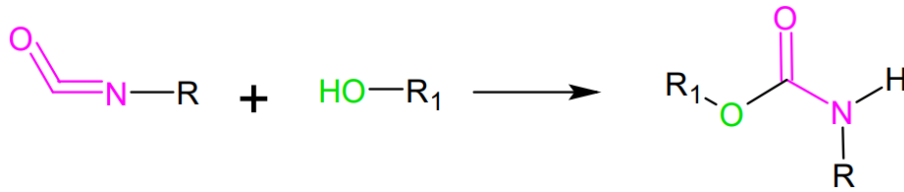


**Figure 4.** General reaction between an isocyanate (purple) and hydroxyl (green) groups for getting urethane group.

PUs began to acquire a particular interest from an industrial, academic and biomedical point of view as smart materials due to their low cost, easy processing, light weight, biocompatibility and SME. In fact, those who are able to reproduce that last characteristic are called *shape-memory polyurethanes* (SMPUs). Figure 5, illustrates some of the most important types and also examples of their uses.<sup>10, 11</sup>

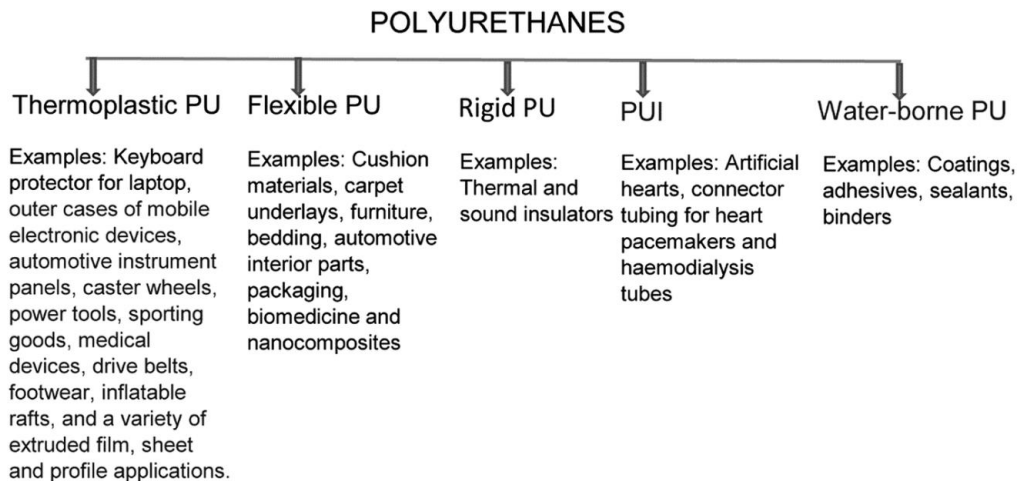


**Figure 5.** Example of PUs uses and applications depending on type.<sup>9</sup>

Thermoplastic PUs (TPUs) are flexible with good resistance to impact, abrasion and weather.<sup>12</sup> Flexible PUs (FPU) comprise some block copolymers whose flexibility is based on the phase separations between the soft and hard segments. A combination of these properties can ensure a good flexibility in PU compounds. Rigid PU represent one of the most commonly known insulation materials used in windows, walls or roofs. The presence of ionic groups in polyurethane ionomers (PUI) backbone chain has many advantages, such as better dispersion in polar solvents due to their enhanced hydrophobicity and improved thermal and mechanical properties.<sup>13</sup> Coatings and

adhesives that make use of water primarily as solvent are often referred like waterborne polyurethanes (WPU). There are several legislation that place restrictions on the amount of allowed volatile organic solvents and other hazardous air pollutants that may be released into the environment. Some commercial and industrial applications are therefore dependent on polyurethane dispersions (PUDs), or waterborne polyurethane dispersions (WPUDs).<sup>14</sup> It is difficult to extensively explain all the applications this polymer has, therefore, as this work will be focus on the textile applications of SMPUs next sections will explain the process for getting them.

The procedure for obtaining the textile from SMPUs start producing *shape-memory fibres* (SMFs). Fibres can be get using *wet*, *dry*, *electrospinning* and *melt* spinning methods, each of them chosen depending on the characteristic of the polymer. First time used in the late 19<sup>th</sup> century wet spinning was one of the original methods for producing synthetic fibres.<sup>15</sup> In this method (*Figure 6 A*), the polymer is dissolved in a suitable solvent and then directly get into a coagulation bath for fibre precipitation. Dry spinning, has many basic principles in common with wet spinning, since in both methods solvents are used. However, the differences are that solidification is achieved more easily through solvent evaporation, which must be highly volatile and no coagulation bath is required. Electrospinning (*Figure 6 B*), consists on a capillary tube or syringe loaded with polymer solution, a metal collecting screen, and a high voltage supply. A polymeric droplet at the tip of the needle is subjected to an electric field in the kV range, deforming into a Taylor cone shape to form a liquid jet. Then, with solvent evaporation, ultrathin fibres are deposited on a collecting screen. Last method, melt spinning (*Figure 6 C*) is a process in which polymer granules are melted inside the extruder, then filaments are hastily solidified.<sup>15,16</sup>

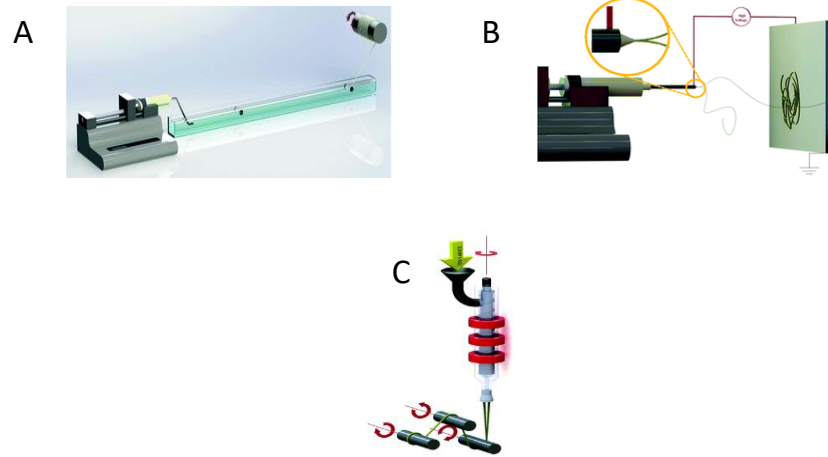


**Figure 6.** Equipment use for wet (A), electrospinning (B) and melt (C) methods for fibre processing. <sup>15,16</sup>

In general, SMFs (Figure 7 A) cannot be directly use for textile applications because of its tactility, to solve that problem, textile finishing process has to be applied. This process is the last step before the fabric reaches the customer, designed to increase attractiveness and serviceability of textile products. This process is done knitting a guide made of wool (Figure 7 B), afterwards, the fibres are added on it by interlocking yarns getting the textile (Figure 7 C). <sup>17</sup>

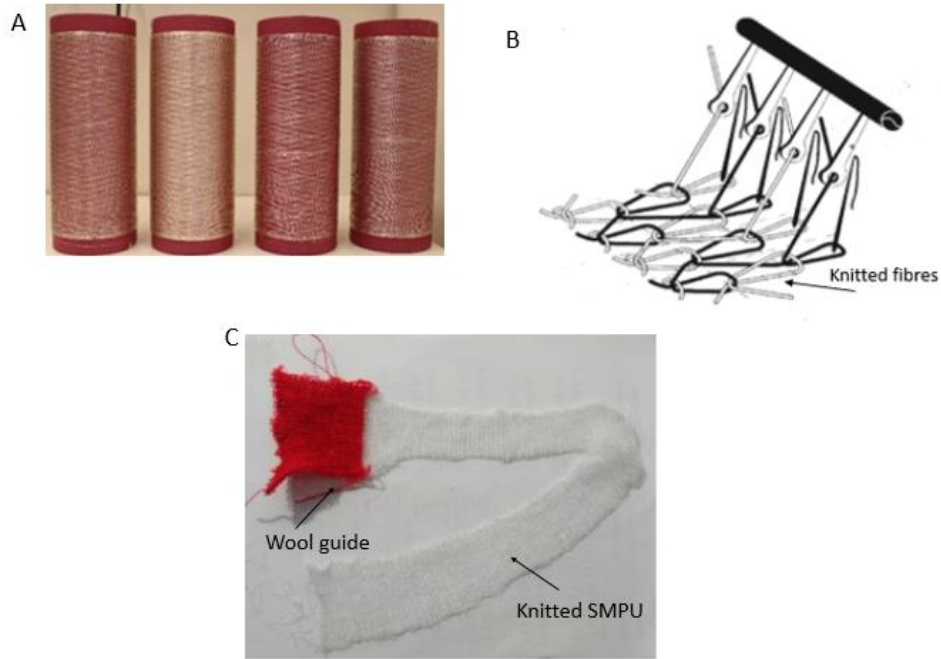


**Figure 7.** Obtained SMFs (A), knitting process interlocking fibres (B) and textile made with SMFs (C).<sup>17,18</sup>

Textile can be produced using *warp* or *weft* knitting methods.<sup>19</sup> Starting with warp method, yarn interlocking is done in a cyclic shape machine, where fabrics are made in spiral configuration around the cylinder allowing needles to produce parallel rows of loops which are interlocked in a zigzag pattern (*Figure 8 A*). Whereas, weft knitting is designed in equipment where yarns run horizontally, from side to side, across the width of the fabric creating loops horizontally that build on top of each other (*Figure 8 B*).<sup>20</sup>

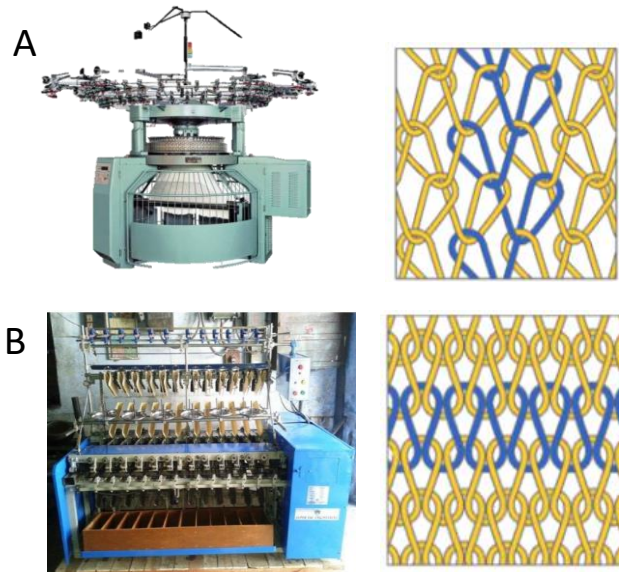


**Figure 8.** Cyclic knitting machine showing in blue zigzag warp pattern (A) and horizontal knitting equipment showing weft blue cross section pattern (B).<sup>20</sup>

Once the material is been processed, it has to be characterized to determine its properties. SMFs and textile characterization is done studying thermal and mechanical methods, explained later in *3.3. characterization Chapter*. However for textile, permeability and tensile testing additional characterization methods have to be applied. Permeability behaviour is analysed using *Water Vapour Transmission Rate (WVTR)* showing in *Figure 9 A*. This technique indicates the amount of water vapour that can permeate per unit area of the packaging material and time, measured in  $\text{g mm/m}^2 \text{ day}$ .<sup>21</sup> *Permeability Oxygen Measurements (PO<sub>2</sub>)* test determines the amount of oxygen through PUs in ‘barrer’ units.<sup>22</sup> Finally, *Figure 9 B* exhibit the equipment for tensile test, this technique applies an uniaxial force to the sample up to the point of yield breaking ( $\text{N}\cdot\text{mm}^{-1}$ ).<sup>18</sup>

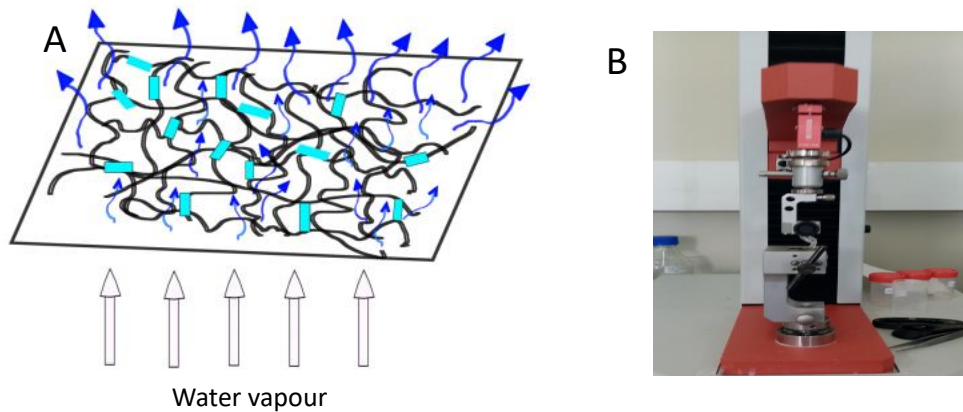


**Figure 9.** Representation of WVTR method displaying water vapour through the textile (A) and tensile test equipment (B) .<sup>18</sup>

The main objective of producing SMFs is to apply them in textile industry to obtain *smart materials*. These kind of smart, intelligent or adaptive systems are those capable of modify significantly one or more properties under controlled conditions. In other words, in response to specific stimulus, they can change their physical properties in a specific manner.<sup>4</sup>

Smart materials have triggered the interest of researchers for a long time, making the research on such materials grow progressively. Thinking on making the sensorial properties of an object variable and interactive, several classes of materials become more interesting than others. It is specially the case for colour changing, light-emitting and shape changing materials. An example are photochromic materials, which have been applied in sunglasses changing lens colour under the exposition of solar radiation (Figure 10 A), or thermochromic materials which behaviour is explained with mugs (Figure 10 B) changing colour when a hot liquid is inside it.<sup>23</sup>



**Figure 10.** Picture of photochromic glasses (A) and thermo-chromic mugs.<sup>23</sup>

SMPUs have also been studied to use as smart material due to the SME they possess, therefore, they have been incorporated in layers contiguous to fabrics. *Diaplex* (*DIAPLEX, SMP Technologies Inc. originally from Mitsubishi Heavy Industries*)<sup>23</sup> claims that has manufacture a membrane itself preserves comfortable conditions by felling the temperature. If body temperature is bellow  $T_{Trans}$  the membrane solidifies maintaining inside the clothing water molecules such as sweat avoiding losing heat (*Figure 11 A*). However, when body temperature is above  $T_{Trans}$ , thermal motion of the molecules forms gaps in the structure, allowing the permeability of water molecules to go throu clothing (*Figure 11 B*).<sup>24</sup> Its most distinctive moisture permeability feature makes it a promising material to use in sports activities such as swimsuit, sneakers or full-fledged mountain activities but also in various other lifestyles, like in underwear or T-shirts.

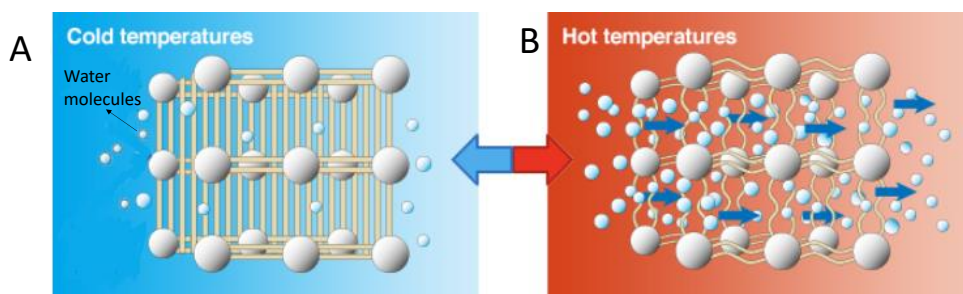


**Figure 11.** *Diaplex* membrane mechanism by which moisture permeability changes with temperature bellow  $T_{trans}$  (A) and above  $T_{trans}$  (B).<sup>24</sup> (Edited Figure)

After taking a look to processing methods and PUs applications, next step requires to synthesise them in order to be able to get in previously explained applications. PUs synthesis can be done following prepolymer, quasi-prepolymer and one-shot methods. Prepolymer method (*Figure 12*) consist in two different phases, firstly the oligodiol and diisocyanate react getting a structure with free terminal -NCO groups called prepolymer and then, the chain extender (CE) is added getting PU. This method, do not require the use of catalys which could produce to get unwanted structures. Quasi-prepolymer method follows the same steps explained in the previous method, however, is synthesised in presence of a large excess of isocyanate. Finally, one-shot method is done in one step, mixing efficiently all reagents during a short time.<sup>25</sup>

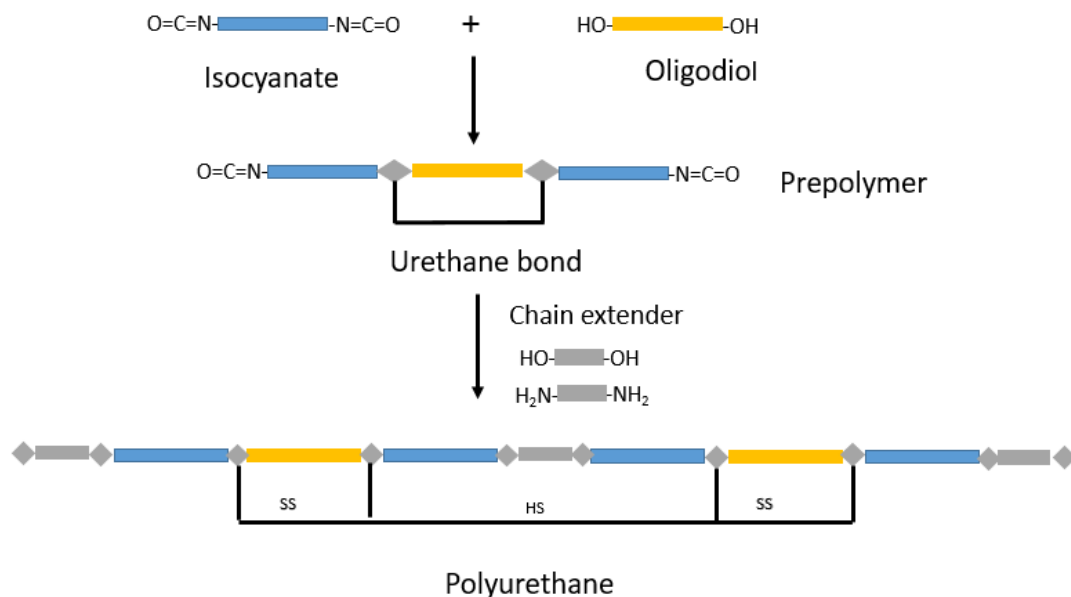


**Figure 12.** Schematic general prepolymer method for PU synthesis showing in blue isocyanate, in yellow diol, grey chain extender and rhombus representing the urethane bonds HS and SS.

Whatever it is the synthesis method used for PUs preparation, it is important to observe some precautions such as working in an inert atmosphere and avoid the presence of water or humidity during polymerization reactions. These two features are important due to the high reactivity of the isocyanate group with water. In the prepolymer method, the most important step is the addition of the hydroxyl and isocyanate groups to get



urethane. However, the residual water of other reactives could react with the isocyanate groups forming carbamic acid, which is an unstable molecule, splitting up into carbon dioxide and amines. For that reason water must be totally erased when the synthesis is performed.<sup>26</sup>

During the work, it has been mentioned that SMPUs have the ability of making previously explained SME. In order to understand the reason of it, a closer look to its structure has to be taken. PUs are synthesised connecting urethane bonds through the aggregation of *hard segments* (HS), which are dispersed in the *soft segments* (SS) matrix. These two segments create a microphase separation since they are not soluble one inside the other.<sup>27</sup> In the structure of *Figure 13 A*, it is observed how the HS of a chain tends to interact with neighboring rigid segment chains, while flexible SS is tangling among itself giving place to a biphasic structure. The interactions between the molecules of the HS increase phase separation between soft-hard segments and enhance the ability of performing the SME.<sup>28</sup>

In *Figure 13 B*, the composition of each segment, as well as the features are exhibited. The SS is formed by high molecular weight polyol which provides softness, flexibility and mobility. Owing to the flexibility this segment has, SMPUs are able to be deformed and then recover the initial shape, or what is the same, they are able to make the SME. On the other hand, the HS is made by the reaction between the isocyanate and CE, providing toughness and stiffness to the polymer.<sup>29,30</sup> These two reactives interact with hydrogen bonds (H-bonds) and dipole-dipole interactions through (–C=O) carbonyl and (–NH) amino groups belonging to the urethanes of close chains becoming a rigid and immobilized segment.<sup>31,30</sup> Depending on the isocyanate used, the HS can be crystalline or non-crystalline. For knowing that, the sample has to be heated above  $T_{Trans}$  and check if it shows a  $T_c$  and  $T_m$  peaks. From a mechanical point of view the increase of HS, makes Young's modulus and glass transition value to increase, while deformation value will be decreased as the polymer has less ability to move.<sup>27</sup>

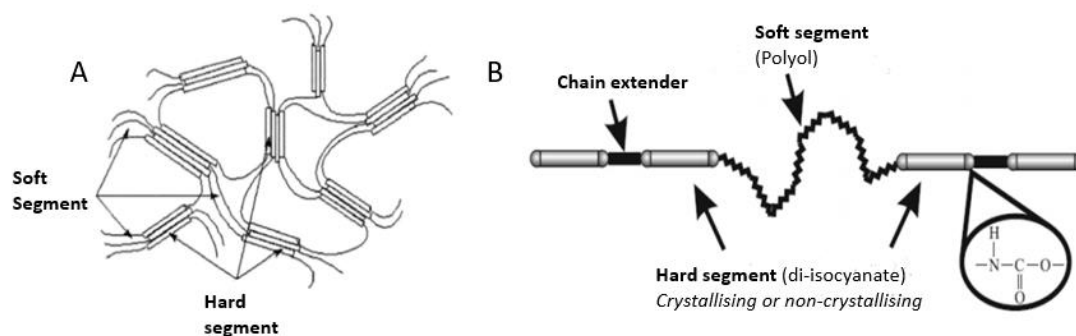


**Figure 13.** Schematic HS and SS micro phase separation of PUs (A) and representation of them in PU chain.<sup>25,29</sup>

It is really important to choose adequately all the reagents that will be used for the synthesis since PUs final features can be change. Starting with the *polyol*, this molecule consists of two or more hydroxyl group units (-OH) with a weight interval between 400-5000 Da.<sup>32,33</sup> The most commons polyols use for the synthesis are polyethers, polyesters, polycarbonates and polybutadiene diols. Polyethers are principally used in rigid and semi-rigid foams, whereas polyesters in elastomers, textile and lining.<sup>34</sup> Depending on the final characteristics, the molecular weight has to be taken into account. If the polyol has a low molecular weight (few hundred molecules), hard plastics are made, whereas, high molecular weight (around ten thousand units and above), produces flexible polymers.<sup>9,34</sup>

Next reactive required is the isocyanate (-N=C=O). These molecules are highly reactive substances that give addition reactions through -C=N binding with alcohols, water and amines.<sup>34</sup> For PUs synthesis usually di, tri or polyisocyanates are used,<sup>35</sup> among the most used can be found toluene-2,4-diisocyanate (TDI), diphenilmethane-4,4-diisocyanate (MDI), hexamethylene diisocyanate (HDI) and isophorone diisocyanate (IPDI).<sup>36</sup> PUs synthesis is easier using aliphatic rather than aromatic isocyanate molecules, since aromatic compounds are really stable turning out to have lower reactivity. However, aromatic isocyanates show better mechanical properties getting higher values of stiffness,  $T_g$  and  $T_m$ .<sup>35</sup> In order to understand that effect, the chain chemical structure has to be analysed. The  $T_g$  value has been foresight using two parameters, chain

flexibility and reagents volume choosing as an example HDI and MDI isocyanates. Comparing both structures MDI is an aromatic compound containing two phenyl groups making more stable and bulkier compound than HDI which is linear aliphatic molecule. Due to MDI structure, the chain will be stiffer meaning that amount of temperature that requires to move the chain is higher than with aliphatic linear compound. Therefore, from a mechanical point of view aromatic compounds seem to be the best type of molecules, nevertheless, a toxicology evaluation shows that they are toxic breaking down to mutagenic and carcinogenic compounds when they are degrade.<sup>35</sup>

Last reactive used is known as chain extender (CE). They are used to extend the prepolymer getting larger macromolecular units bonding with free  $-NCO$  groups.<sup>31</sup> These molecules usually are low molecular weight diols or short diamines such as 1, 4-butanediol (BD) or diethylamine.<sup>30</sup>

Environmental problems and public concern about climate change are promoting the use of bio-resources derived from animals or plants. Environmental friendly polymeric biocompatible materials have been getting a great attention for their use in different research fields in order to replace petroleum-based polymers.<sup>31</sup> Biocompatibility is the absence of allergic and immunity reactions between some materials and organic tissues, in other words, the material must cure and/or reproduce a biological function. Polymeric compounds have been used in lots of medical devices, for instance in 1937 methyl polymetacrylate (PMMA) was first polymer used in odontology prosthesis or polyethylene terephthalate (PET) was clinically identified for synthetic vascular prosthesis.<sup>35</sup>

PUs can be obtained from petroleum sources using high energy and creating environmental issues. However an eco-friendly alternative is been proposed using natural resources such as natural vegetable oils. These oils consist on triglyceride esters of fatty acids, joined by a glycerol molecule with reactive sides, such as carbon-carbon double bond, ester and hydroxyl group (*Figure 14*).<sup>31</sup> Among vegetable oils such as Tung/Chinese Wood oil, soya, sunflower, corn, rapeseed, colofonia/ gum rosin,<sup>31</sup> castor oil (CO) appears to be a good CE for providing biocompatibility feature to PUs.<sup>37</sup>

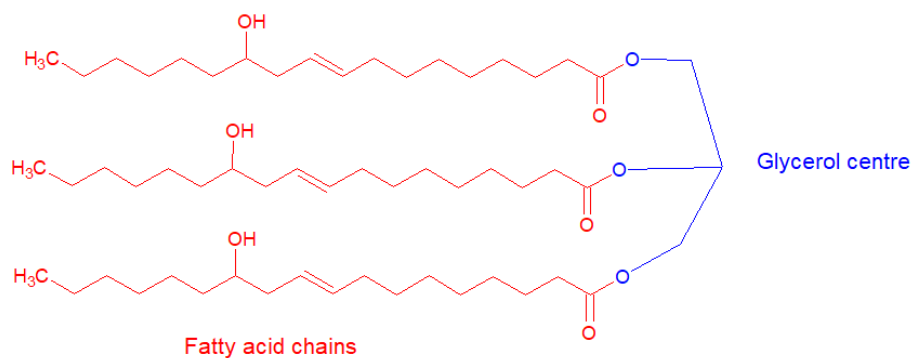


**Figure 14.** Castor oil molecular structure showing in blue glycerol centre and in red fatty acid chains.

CO is obtained from castor bean seed of *ricinus communis* from *euphorbiaceae* family (Figure 15 A). The fatty acid contains seed 40-60% (Figure 15 B), where 90% is ricinoleic acid (12-hydroxy-9-octadecenoic acid) containing in the twelve carbon a hydroxyl group useful for PUs preparation.<sup>37,38</sup> Castor oil has been studied in outnumber publications related with PU synthesis, which shows a wide range of physic-chemical features depending in the amount of CO used and the isocyanate chosen.<sup>31</sup>

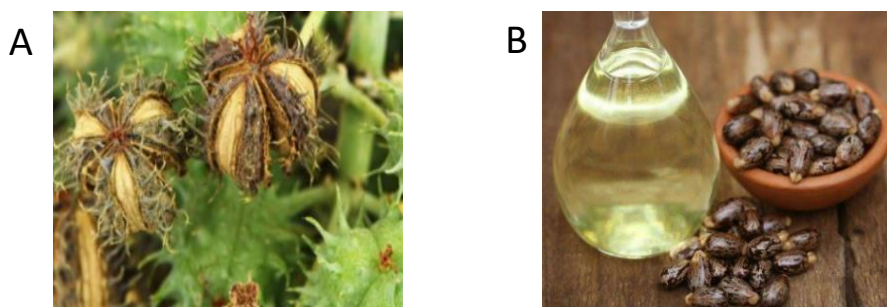


**Figure 15.** *Ricinus Communis* plant (A) Castor oil and seeds (B).<sup>38</sup>

One of SMPUs challenge is to get good physical-chemical and biocompatibility properties in order to use in medical devices. For instance, SMPUs have been suggested to work like stent to avoid thrombosis.<sup>39</sup> This disease produces a blood clot in blood vessels, also known as a thrombus, which is composed of platelets and fibrins. This clot can block or obstruct blood flow in the affected area, causing serious complications if the clot moves to a crucial part of circulatory system, such as brain or lungs.<sup>39</sup>

In *Figure 16* there is an example of thrombosis disease in legs. At first, the vein shows a normal blood flow since the platelets (red circles) go through the leg. However when blood starts coagulating, the amount of flow going through it is slightly decreased. That state is known as deep vein thrombosis stage. From that moment on the flow will be decreasing more and more until the total inhibition it. SMPUs can be used as stent and preprogrammed to activate at a body temperature changing its size, preventing this disease without a need of auxiliary devices (catheter) or implanting medical devices that often require complex surgery.<sup>40</sup>

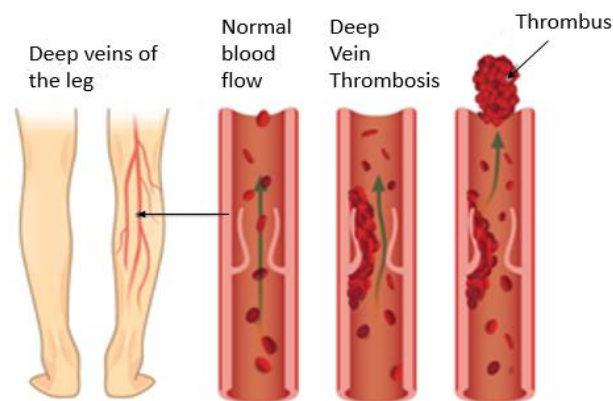


**Figure 16.** Legs thrombosis disease representing the decrease of blood flow due to thrombus formation.<sup>41</sup>

## 2. OBJETIVES

The objectives of this work are the synthesis and characterization of thermoresponsive SMPUs with applications in textile industry. To achieve this and based on previous works,<sup>42,43</sup> an improve in physical-chemical properties have been seek. Therefore, poly (tetramethylene ether) glycol at three different molecular weight, isophorone diisocyanate (IPDI) and castor oil (CO) reagents have been used, at three different stoichiometric NCO/OH ratios, to synthesise the different polymers. In addition, biocompatibility feature has been added to SMPUs using CO as chain extender, in this way aiming to improve their non-toxicity.

### **3. DEVELOPMENT**

#### **3.1. REAGENTS**

Three reagents have been used for PUs synthesis: ether-type polyol, a cyclic non-aromatic isocyanate and a chain extender. The polyol used has been poly (tetramethylene ether) glycol, also known as polytetrahydrofuran (PTMG) at three different molecular weights 1000 (PTMG 1000), 650 (PTMG 650) and 250 (PTMG 250)  $\text{g}\cdot\text{mol}^{-1}$ . The isocyanate used has been isophore diisocyanate (IPDI), which is aliphatic and it has  $222.3 \text{ g}\cdot\text{mol}^{-1}$  molecular weight and a density of  $1.062 \text{ g}\cdot\text{cm}^{-3}$ . Last reactive has been Castor oil, which has a molecular weight of  $933.4 \text{ g}\cdot\text{mol}^{-1}$  and a density of  $0.961 \text{ g}\cdot\text{cm}^{-3}$ . All reactives have been purchased from Sigma Aldrich commercial house.

Changing the composition of these three reagents, SMPUs with different properties are going to be synthesised changing hard-soft segment proportions until the optimal value for its applications is found.

#### **3.2. SYNTHESIS**

All polyurethanes were synthesised using prepolymer method through this mechanism (*Figure 17*). In the first stage of the method, PTMG (blue) and IPDI (green) are mixed in a five neck reactor (250 mL) heating in an oil bath at  $70^\circ\text{C}$  during 2 hours at 250 rpm in an inert media using  $\text{N}_2$  to get the prepolymer. After two hours, in the second stage, previously dried at  $80^\circ\text{C}$  during 18 hours CO (black) is added using previous conditions but stirring for 10 more minutes getting SMPU.

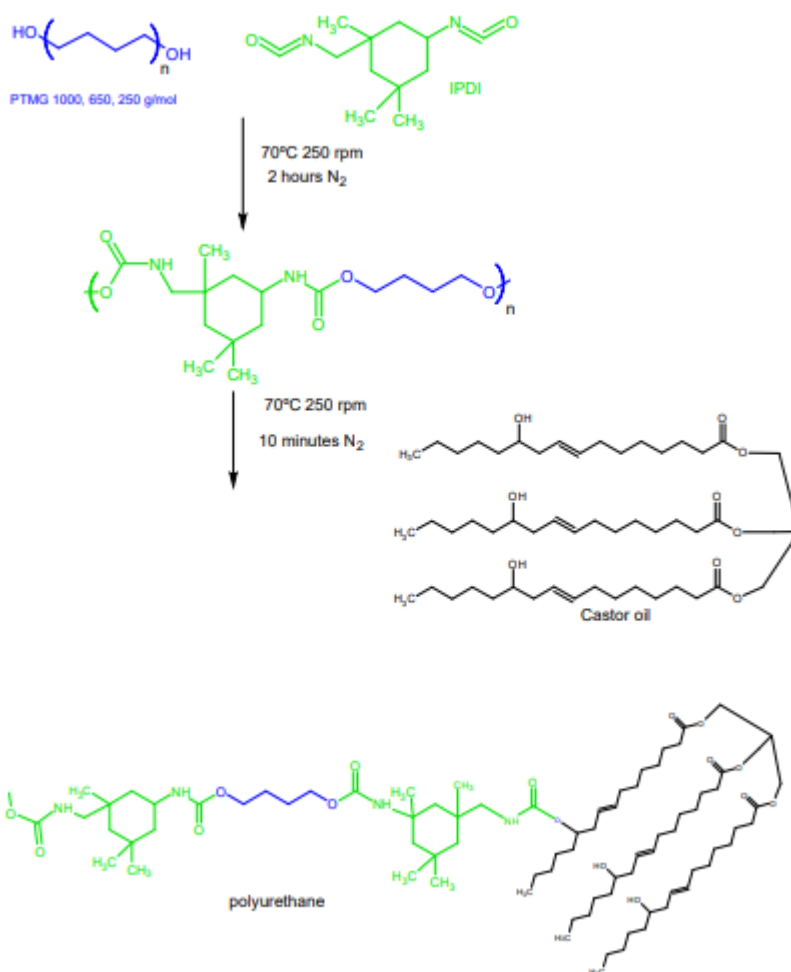


**Figure 17.** Synthesis of the studied PUs by Prepolymer method.

Once the reaction time was completed, from inside the setup of *Figure 18 A* a viscous product was collected which is poured into metal moulds (50 mm x 50 mm x 1.5 mm). Right after, the metal moulds are got into a hydraulic press (*Figure 18 B*) where the polymer is brought down at 100 kg·cm<sup>-2</sup> pressure at 100°C for 24 hours (*Figure 18 C*). The stoichiometry ratio N, has been upward from N= 4 to N= 6 to increase HS proportion in each synthesis. Values bellow N= 4 have been dismissed since too sticky polymers were getting, making difficult their characterization.

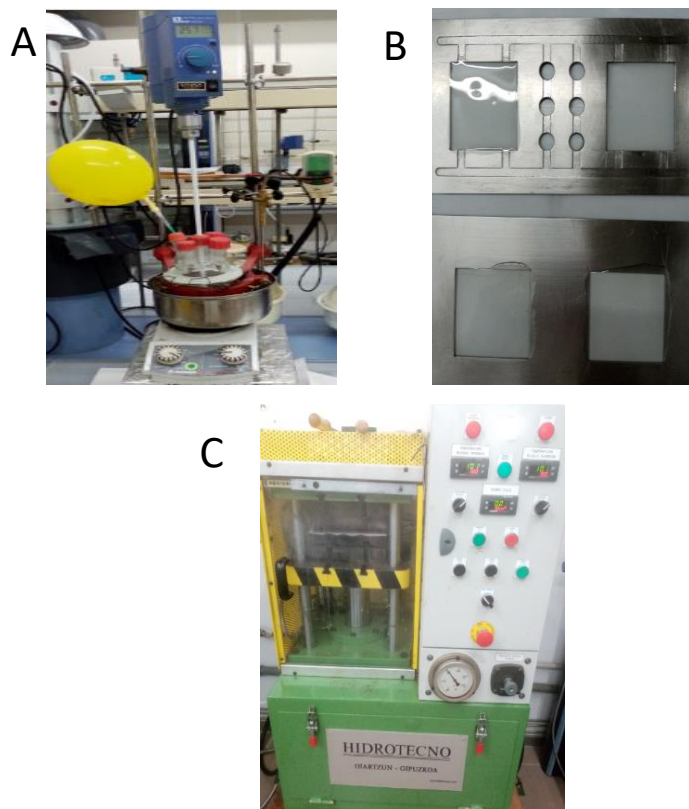


**Figure 18.** Set up for PUs synthesis (A), polymer poured into metal moulds (B) and insertion into the press (C).

In previous procedure 35 g of product were obtained, however, in order to get the fibres at least 150 g were required. It is therefore, the polymer is poured into silicone moulds and get inside the muffle set at 100°C during 24 hours without applying any pressure (Figure 19 A).

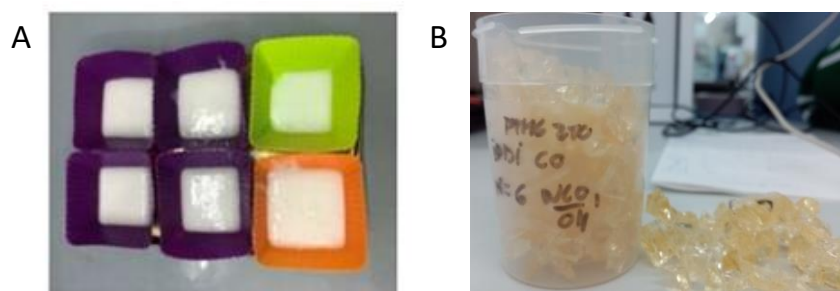


**Figure 19.** PUs moulds after been in the muffle (A) and PUs moulds cut into small pieces for getting into the extruder (B).



After 24 hours, PUs are removed from the muffle and cut into small pieces (Figure 19 B) for sending to IK 4 Tekniker technological centre (Tekniker member of Basque research & technology alliance) in order to make fibres. The small polyurethane pieces were inserted into coned shaped doble screw extrusion machine (Figure 20) (Thermo-scientific-Haake-minilab II) following next procedure. First, the small polymer pieces are get into 0.35 mm tolva where are heated at 175-180°C and 15 rpm velocity. Straightaway, the polymer is get out from the shapping dye in thread way,where is freezed using cold air. Last step requires to gather the them around a bobbin getting 0.5 mm diametre fibre.

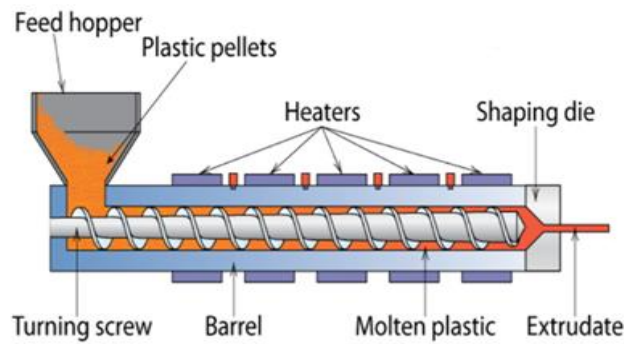


**Figure 20.** Scheme of an extrusion process exhibit all parts inside it. <sup>15</sup>

After the process of making fibres, they are knitted in order to get textile. Knitting was performed in a LK-150 knitting equipment (Figure 21 A) in weft mode. The initial step of the process requires to knit a guide, which it was made using wool of 0.35 mm thick. Afterwards the polymer is added above the knitting guide like is shown Figure 21 B.

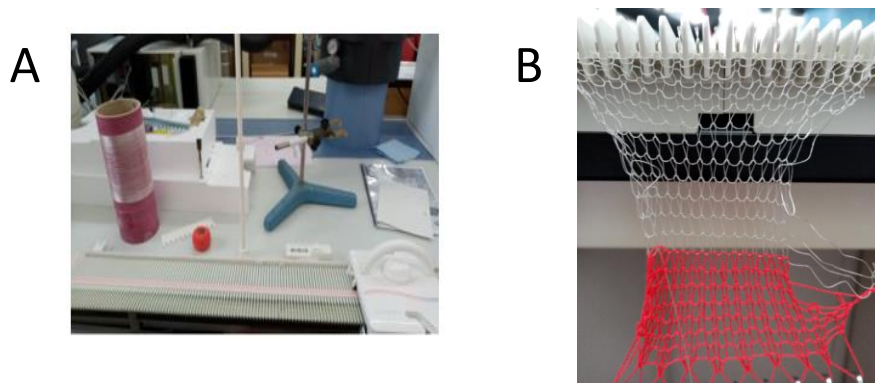


**Figure 21.** LK-150 knitting equipment (A) and textile made from PU (B).

### 3.3 CHARACTERIZATION

Characterization techniques are used to find out physical-chemical properties of synthesised materials, assuring the material is adequate for required purpose. In this case, the HS was used to control the final properties of the material. Technique used have been *Attenuated total reflection-Fourier transform infrared spectroscopy* (ATR-FTIR) for monitoring the reactions and to confirm that the isocyanate groups were completely reacted; *thermogravimetric analysis* (TGA) to determine initial degradation temperature ( $T_i$ ) as well both segments percentages. By means of *differential scanning calorimetry* (DSC) and *dynamic mechanical analysis* (DMA) glass transition temperature is calculated, while, *thermomechanical analysis* (TMA) was carried out to examine SME.

#### 3.3.1 Attenuated total reflection-Fourier transform infrared spectroscopy

*Attenuated total reflection-Fourier transform infrared spectroscopy* (ATR-FTIR) was used to follow the reaction between the diisocyanate and hydroxyl groups.<sup>44</sup> Infrared spectra were collected on a Nicolet Nexus FTIR spectrophotometer (*Figure 22*). Spectrums were obtained using ATR tool from  $500$  to  $4000\text{ cm}^{-1}$  range at  $4\text{ cm}^{-1}$  resolution and 32 scans per spectrum.



**Figure 22.** Attenuated total reflection-Fourier transform infrared equipment.

### 3.3.2 Thermogravimetric analysis

*Thermogravimetric analysis* (TGA) is used to find out samples thermal stability. The process is done through depolymerization of functional groups or linkages present in the polymer chain, measuring loss weight through a thermal treatment in a period of time.<sup>45</sup> There are many depolymerization mechanisms such as, hydrolysis (breakage of a polymer by reacting with water producing two or more molecules of other substance), thermolysis (chain rupture reactions that occur by warming up), oxidation (reactions with oxygen), pyrolysis (transformation of one substance into another by heat reactions exclusively without oxidation) and solvolysis (degradation produced by solvents).<sup>34</sup>

10-20 mg samples were weight in *TA-60 Shimadzu thermobalance* (*Figure 23 A*) while TGA analysis was performed using *TA-60 WS thermal analyser* heating at  $10^{\circ}\text{C}\cdot\text{min}^{-1}$  from  $25\text{-}800^{\circ}\text{C}$  under a nitrogen flow ( $20\text{ mL}\cdot\text{min}^{-1}$ ). In *Figure 23 B* it is observed a model thermogram. Data from the black line shows the percentage of weight loss during a period of time. From it, the information acquire is the initial thermal stability temperature ( $T_i$ ) set at 2% of degradation and also the weight of HS-SS percentages. While from red line, the first derivative is calculated to know the temperature of the maximum temperature degradation peak ( $T_D$ ) which is related with each segment.

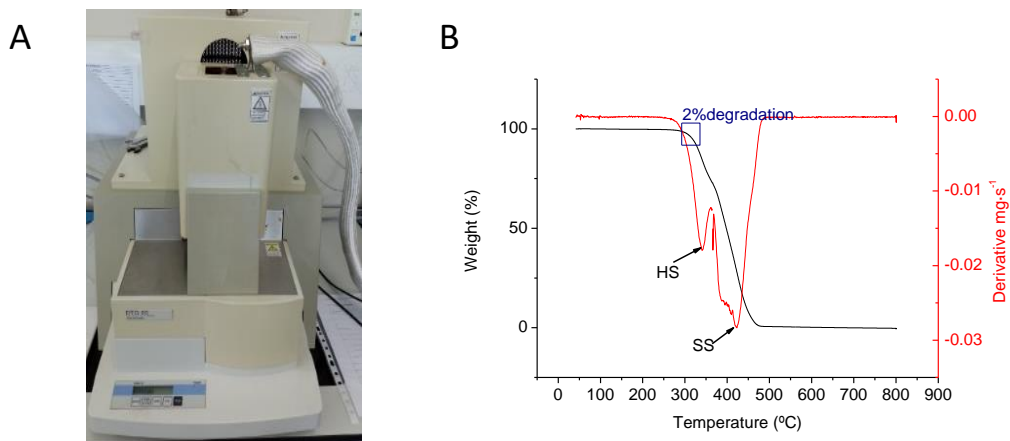


**Figure 23.** Picture of Thermogravimetric analysis equipment (A) model thermogram (B) in black  $T_i$  and in red derivative showing each segment.

### 3.3.3 Differential scanning calorimetry

Differential scanning calorimetry (DSC) is the most frequent technique use in thermal analysis. DSC uses temperature and heat flux associating them to a polymeric transition in function of time or temperature, acquiring quantitative and qualitative endothermic and exothermic values during the physical-chemical transitions.<sup>46</sup> Measures are done comparing heat flux difference between the sample and reference, showing heat difference when a sample takes up or frees heat due to fusion, crystallization, chemical reactions, polymorphic transitions, vaporization and glass transition temperature.<sup>47</sup>

DSC analysis were performed in METTLER TOLEDO 822° (Figure 24 A), samples weight between 10-14 mg are get inside a capsule closing hermetically and inserted into the analyser subjected to consecutive heating and cooling periods. In the first period, the sample is heated from  $-100^{\circ}\text{C}$  to  $250^{\circ}\text{C}$ , then in the second period, is cooled down from  $250^{\circ}\text{C}$  to  $-100^{\circ}\text{C}$  and in the third period is reheated again from  $-100^{\circ}\text{C}$  to  $250^{\circ}\text{C}$  (Figure 24 B). In the second heating the  $T_g$  value is calculated from the extrapolation of the tangent to the curve presented in the inflection zone (Figure 24 C). The process is done at  $10^{\circ}\text{C}\cdot\text{mL}^{-1}$  velocity with a nitrogen flux of  $50\text{ mL}\cdot\text{min}^{-1}$ .

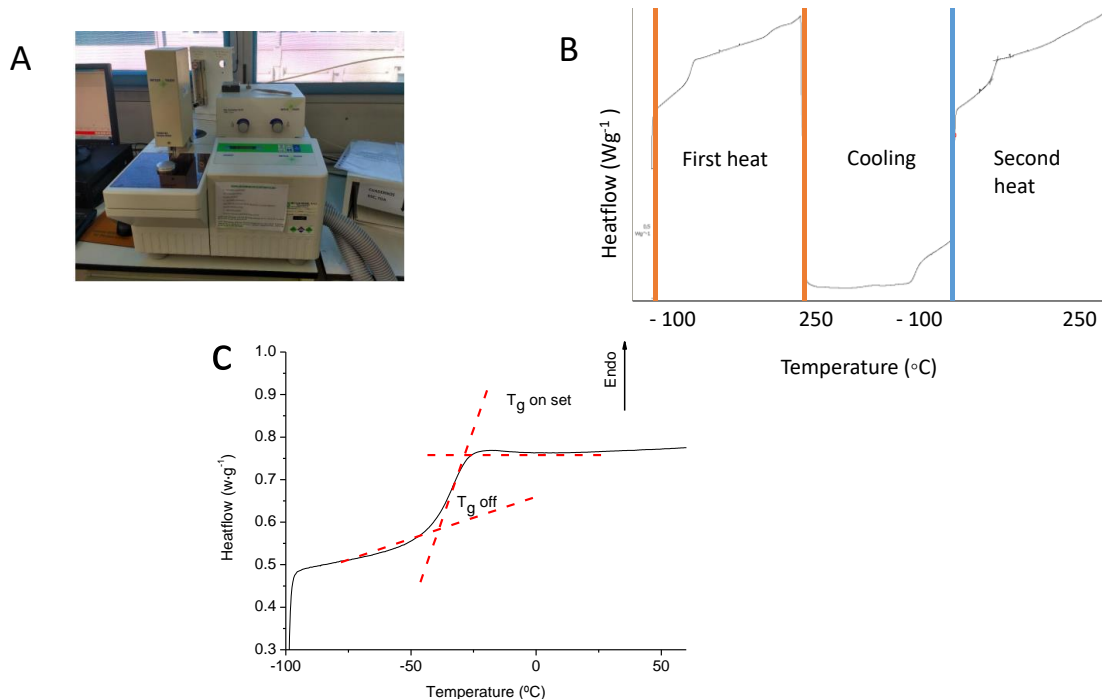


**Figure 24.** DSC Mettler Toledo analyser equipment (A), DSC thermogram programming method (B) and tangent extrapolation for  $T_g$  calculation (C).

### 3.3.4 Dynamic mechanical analysis

*Dynamic mechanical analysis* (DMA) is the most important technique for measuring mechanical and viscoelastic properties of thermoplastic, thermosets, elastomers, ceramics and metals. With this technique, the sample is subjected to a periodic stress in one or several different deformation modes (bending, tension, shear and compression). The *module* is measured in periodic function of time or temperature providing information of phase transition.<sup>48</sup>

*Young's dynamic complex module* ( $E^*$ ) is calculated adding the *storage module* ( $E'$ ) and *loss module* ( $E''$ ). The storage module ( $E'$ ) quantifies the energy stored elastically by the material upon deformation, and provides information regarding the stiffness of the material. Whereas loss module measures losing energy in heat way. The relation between both modules is known as *loss factor* or *loss tangent*  $\text{Tan}\delta = E''/E'$ .<sup>26,8</sup>

In *Figure 25 B* it is represented a model DMA thermogram, showing in the right the  $\text{Tan}\delta$  and in the left  $E'$  while temperature is increasing. The thermogram, is going to be divided

in three parts where  $E' > E''$ ,  $E' = E''$  and  $E' < E''$  to explain it. First the  $E'$  value is higher than  $E''$  because temperature is below  $T_g$ . Due to that, the sample is stiff storing energy as it has not ability to move. That is seen as  $E'$  value maintains constant and  $\text{Tan}\delta$  value is increasing. Then the temperature will keep on increasing until  $E' = E''$ . In that moment the value corresponding to the  $T_g$  is get, as the sample from been rigid becomes rubbery getting the maximum  $\text{Tan}\delta$  value. From that moment on, chains can move since temperature is higher than  $T_g$ . Therefore, all the energy that the sample has been storing is release in heat way. That results in getting higher  $E''$  value than  $E'$ , also observed with a decrease in  $\text{Tan}\delta$  value.

DMA experiments were done on the DMA-1 METTLER TOLEDO analyser (Figure 25 A). In Figure 25 B thermogram,  $E'$  and  $\text{Tan}\delta$  values were recorded in ranges between  $-100^\circ\text{C}$  to  $150^\circ\text{C}$ , 3 K/min heating ranges, 1, 3, and 10 Hz deformation frequencies and 20  $\mu\text{m}$  displacement. The probet used was 1.5 mm x 5.0 mm x and 3.0 mm (thick x length x wide). Even though three frequencies have been used in the experiments, only 1 Hz has been graph in results chapter.

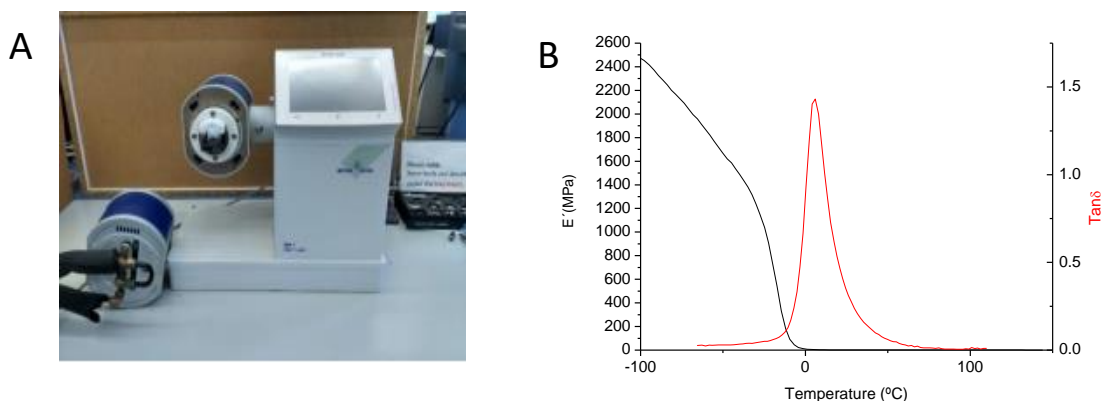


**Figure 25.** DMA-1 METTLER TOLEDO equipment (A) and  $E'$  black and  $\text{Tan}\delta$  1 Hz red values during heating process (B).

From an experimental point of view DSC and DMA measures samples  $T_g$  value, however, exits some differences between each techniques. DSC calculates based on heating and cooling in a static way, while DMA measures mechanical stress which is directly

connected with chain mobility or intermolecular mobility. Therefore, dynamic experiments exhibit higher  $T_g$  than static experiments:  $\text{DMA } T_g > \text{DSC } T_g$ .<sup>49</sup>

### 3.3.5 Thermomechanical analysis

*Thermomechanical analysis* (TMA) studies samples deformation at different temperatures. Knowing that SMPUs are thermally induced SMPs, this technique is used to evaluate the SME.<sup>18</sup> TMA analysis was performed in the same equipment used for DMA technique. To choose the temperature range in which the experiments have been carried out,  $T_g$  results got from the previous DMA analysis were examined. The reason for this is that for watching the SME, the temperature range must be above and below the  $T_g$ .

TMA cyclic process was calculated using the following procedure (*Figure 26*). In the first place, the sample is heated to 100°C for being in a temperature higher than the  $T_g$  without applying any force ( $F=0$  N), then temperature is held for a minute. Afterwards, programming steps begins where a  $F=2$  N is applied while temperature is dropped from 100°C to -50°C, or what is the same, below  $T_g$ . In this part samples maximum stretching is calculated ( $D_{\max}$ ). Right after, the temperature and the force will maintain constant during 30 minutes fixing in its new temporary shape ( $D_{F=0}$ ). After this process, the force is discharged ( $F=0$ ) and the sample is kept in these conditions for 5 minutes. Last step, requires to reheat the sample above the  $T_g$  from -50°C to 100°C to recover the initial shape it got showing the SME ( $D_f$ ).

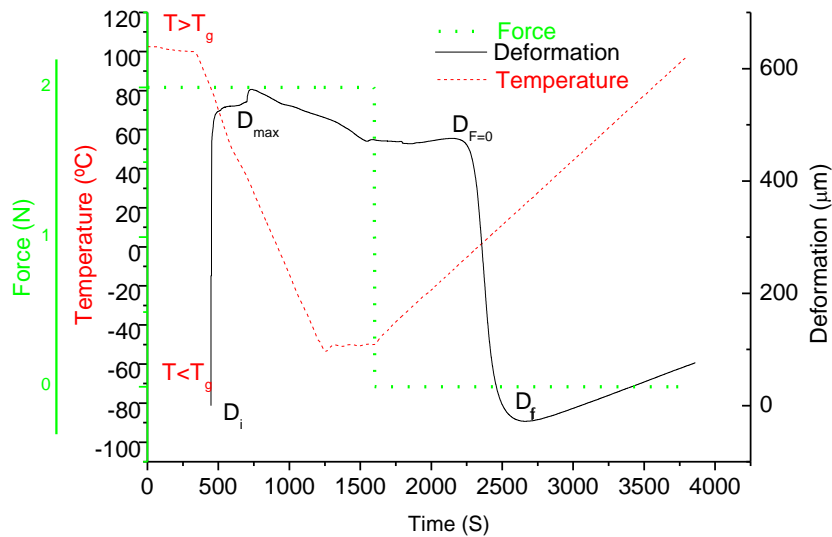


**Figure 26.** Example of thermomechanical cycle SME. In green force, deformation in black and temperature in red applied during a period of time.

These three parameters deformation ( $R_d$ ), fixing ( $R_f$ ) and recovery ( $R_r$ ) are calculated from equation 1-3, using a length of 5 mm in all the samples.

$$\text{Deformation \% } (R_d) = \left( \frac{D_{\max}}{L} \right) * 100 \quad (1)$$

$$\text{Fixing \% } (R_f) = \left( \frac{D_{F=0}}{D_{\max}} \right) * 100 \quad (2)$$

$$\text{Recovery \% } (R_r) = \left( \frac{D_{\max} - D_f}{D_{\max}} \right) * 100 \quad (3)$$

### 3.3.6 Cytotoxic analysis

Cytotoxic examination is defined as cells basic function alteration due to a chemical substance. This process is done using *in vitro* essays to identify potentially hazardous chemicals. The parameter used to quantify the biocompatibility is cell proliferation, which calculates the inhibition of cellular grow, recording cellular harm or dead.<sup>50,51</sup> There are many *in vitro* essays, such as accelerated degradation in saline phosphate buffer or antibacterial PUs trial.<sup>52</sup> Despite all of them, MTS calorimetric essays has been used for biocompatibility analysis. This method is based in the colour change of (3-(4,5-dimetiltiazol-2-il)-5-(3-carboxymetophenyl)-2-(4-sulfophenyl)-2H-tetrazoile or MTS salt



which is yellow reactive, in presence of mitochondrial succinate dehydrogenase is reduced into a blue product called *formazan*.<sup>51</sup>

MTS salt is brew in presence of *fenazine metosulphate* (PMS) (5% v/v diluted in a phosphate buffer (PBS) containing  $Mg^{2+}$  and  $Ca^{2+}$ ). This reacts with mitochondrial dehydrogenases producing formazan which shows a maximum absorbance peak at 490 nm in PBS. The generated formazan is proportional to the amount of living cells in a crop (until 150000 cells).

SMPU samples have been cut in 6 mm diameter and 1.5 mm thickness, afterward there were introduced in 96 wells crop. 296 Hek cellules (human kidney embryonary cells) were sow and set at 2000 cells/well density. Afterwards, FBS (Fetal Bovine Serum) was remove from the media adding 20  $\mu$ L of MTS:PMS in each well. After two hours of incubation in MTS:PMS they are measured at 490 nm absorbance.

Biocompatibility study is done controlling cell proliferation after 48 and 72 hours of incubation. From the same SMPU sample, five replicates are prepared to check reproducibility. This test was performed in Basque Center for Biophysics BioFisika in UPV/EHU.

#### **4. RESULTS AND DISCUSSION**

PU's synthesis has been proceed exanimating PTMG at three different molecular weight (1000, 650, 250  $g \cdot mol^{-1}$ ), a cyclic isocyanate IPDI and a natural origin chain extender CO. For this reason, during results presented will use the same name terminology PTMG/IPDI/CO at different N numbers stoichiometry. N value has been increased from N=4 to N= 6, in this way, increasing the HS% in each synthesis. The study begun with the characterization of PTMG 1000-650-250/IPDI/CO at NCO/OH= 1 ratio.

##### **4.1 SAMPLE CHARACTERIZATION AT NCO/OH= 1 RATIO**

First, ATR-FTIR technique *Figure 27* spectra assures that the reagents have form SMPUs. Peaks corresponding to carbonyl group are seen at 1700  $cm^{-1}$  as well C-O-C vibrating peak between 1000  $cm^{-1}$  and 1200  $cm^{-1}$ . Even more, around 1590-1730  $cm^{-1}$  N-H band

and at  $1400\text{ cm}^{-1}$  C-N stretching band are observed. Theoretical PUs bands are shown in *Attachment Table 1S*.<sup>8</sup>

Even though the synthesis have been done at stoichiometry NCO/OH= 1 ratio supposing that all IPDI reacts with PTMG, the peak corresponding to the  $\text{-NCO}$  group is seen at  $2245\text{ cm}^{-1}$  for PTMG 650/IPDI/CO N= 5 and PTMG 250/IPDI/CO N= 4 samples. Taking into account that the isocyanate is the most hazard reactive that has been used, the fact of getting  $\text{-NCO}$  free groups makes to get less biocompatible samples. Even more, since not all of it has reacts leads to have less HS% meaning that the samples are not as stiff as they are supposed to be.

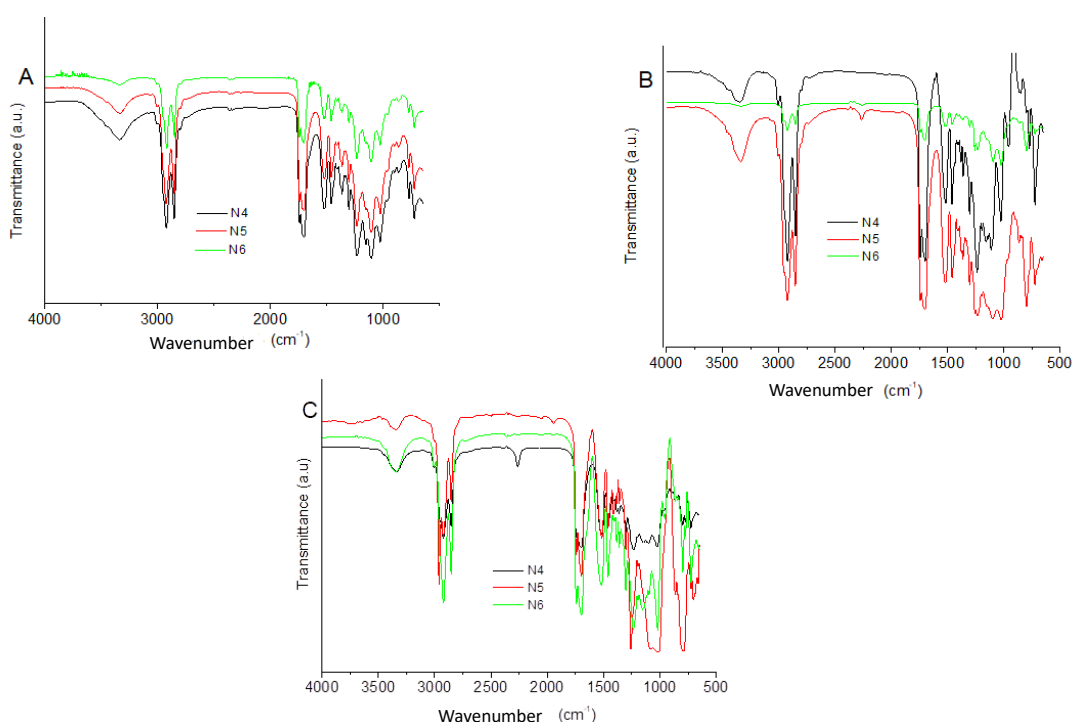


**Figure 27.** ATR-FTIR spectra of SMPUs samples PTMG/IPDI/CO N= 4-6 using different PTMGs values: 1000 (A), 650 (B) and 250 (C)  $\text{g}\cdot\text{mol}^{-1}$ .

Characterization carried on with thermogravimetric analysis in order to evaluate  $T_i$ ,  $T_d$  and HS percentage. In order to explain these three parameters *Figure 28* and data from *Attachment Table 2S* is going to be used.

Starting with the  $T_i$ , it was expected as the N value increases also should the  $T_i$ , because the sample contains more HS proportion. Looking at continue lines in *Figure 28 A*, It is

observed that all samples start degrading at very similar temperatures, same effect is seen for *Figures 28 B* and *C*. This effect has been related to IPDI and CO molecules, since during the synthesis they are bonded from IPDI nitrogen of the isocyanate and CO hydrogen of hydroxyl groups producing H-bonds giving a higher thermal stability to the polymer.

Related with this effect of increasing the N value, it has also been calculated the experimental HS percentage comparing with theoretical HS percentage. In order to quantify the experimental HS%, a slope change should be seen in continue lines. However, both segments appear very close making difficult to know the end of one segment and the beginning of the next. This can be explained with *Figure 28 C N= 6*. The green continue line seems to be utterly straight when it should have a slope change at temperatures between 300-400°C, since at that temperatures appear the maximum temperature degradation peak corresponding to the segments. Due to this, the values get from theoretical HS% and experimental HS% are quite different.

Analysing the derivatives, two maximum degradation peaks should be observed at *Figure 28 A* dash lines, as well for *Figures 28 B* and *C*. First maximum temperature degradation peak ( $T_{D1}$ ) appears around 300°C. First stage of degradation is related to urethane bond decomposition, which takes place through the dissociation to isocyanate and alcohol, the formation of primary amines and a terminal olefinic group on the polyester chain, the formation of secondary amines and  $CO_2$ . While the second maximum temperature degradation peak ( $T_{D2}$ ) appears around 400°C belonging to SS.<sup>37</sup> Furthermore, taking a look to PTMG 1000/IPDI/CO N= 5 and N= 6, PTMG 650/IPDI/CO N= 5 and PTMG 250/IPDI/CO N= 5 samples a third peak is seen. This peak has been associated to a remaining structure, a probable C-C bond cleavage or it could be related to the SS as it appears at a temperature close to it.<sup>53</sup> In order to clarify the new peak, thermogravimetric analysis/ infrared spectroscopy (TGA-IR) techniques has been proposed. TGA is coupled to IR spectrometer to combine thermogravimetric analysis with the identification capability of an infrared spectrometer. Data received from TGA-IR did not give useful information for peak characterization, since bands were

attributed to C-H stretching relating to hydrocarbon small chain molecules. Also peaks corresponding to carbonyl groups and N-H stretching were observed corresponding to the urethane groups.<sup>54</sup>

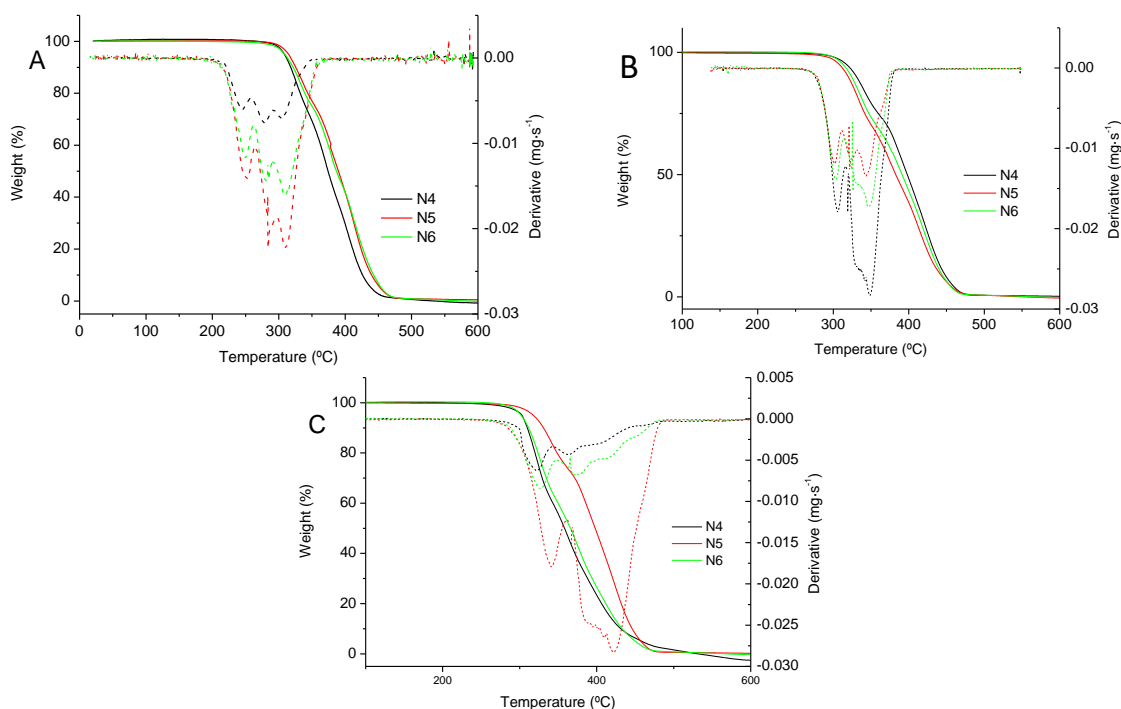


**Figure 28.** TGA thermograms of PTMG/IPDI/CO samples. The continue lines represent the weight loss percentage and dash lines the first derivative for PTMG 1000 (A) PTMG 650 (B) and PTMG 250 (C) form N=4 to N= 6.

The following two characterization techniques, DMA and DSC have been used with the objective of calculating the  $T_g$  value of samples. Starting with results got from DSC analysis (Attachment Table 35), Figure 29 C shows that the  $T_g$  of polyurethanes increases with the HS content, in other words with the N value. It seems reasonable to assume that with N increase, the chain mobility is going to be more restricted each time since the polymer is stiffer requiring a higher need of heatflow for getting rubbery and get the  $T_g$ .<sup>55</sup> Comparing samples using different PTMG molecular weight for a fix N in Figures 29 A, B, C at N= 6, it is observed that the  $T_g$  value is higher for samples containing PTMG 250  $\text{g}\cdot\text{mol}^{-1}$ . That effect happens due to reducing the PTMGs mass, the separation between the micro domains also is reduced, meaning the polymer is losing the flexibility.

Even more, reducing the amount of PTMG also increases the HS% getting a harder and stiffer polymer as there are more H-hydrogen bonds between the HS.

Using DSC technique it has been mentioned that fusion, crystallization and glass transition temperature could be seen. In order to identify those processes, first order and second order transition processes have to be considered. First order transition is seen with peaks going on up and down, generally related to crystallization and fusion processes. The equipment used is *endo up*, that means that the process where heat is absorbed appears an endothermic peak going up (fusion) and process where heat is transmitted show as exothermic peaks down (crystallization). Second-order transition process involves chain movement seen by a slope change from baseline belonging to the  $T_g$ . In *Figure 13 B* of introduction part it was suggested that the HS could be crystalline or not-crystalline, with this technique can be assure if the polymer has a crystalline segment. Taking a look to samples of *Figure 29*, none of them show any first order transition peaks, because there are no peaks going up or down. This means that the HS is not crystalline, or what is the same the polymer is amorphous.

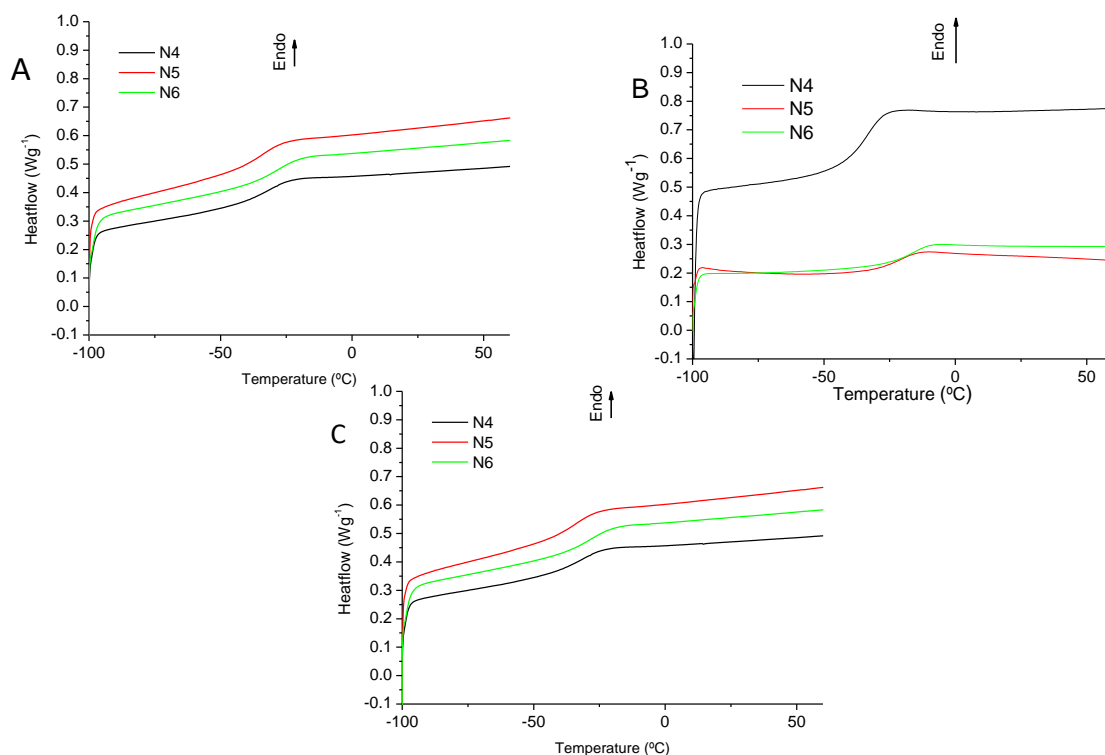


**Figure 29.** DSC calorimetric curves for  $T_g$  examination in samples PTMG/IPDI/CO containing PTMG 1000 (A) PTMG 650 (B) PTMG 250 (C) at different N values.

Using DMA technique glass transition values are calculated as the maximum in  $\tan\delta$ . In Figure 30 B, it has been observed a linear relation between the N value and the  $\tan\delta$  value. Increasing the N values the amount of temperature required to calculate the  $\tan\delta$  value also increases, which is in agreement with the DSC results. With the increased of the N value so it does the HS content meaning that PUs are stiffer. Owing to that, the  $\tan\delta$  line will start increasing at higher temperatures. As the polymer can store energy elastically upon deformation, a higher need of temperature is needed for making the chain rubbery which is related with the  $T_g$ . Also obtained  $\tan\delta$  values have been checked reducing PTMG molecular weight from 1000 to 250  $\text{g}\cdot\text{mol}^{-1}$  for a fix N value. To evaluate this effect N= 6 green sample from Figures 30 A, B and C is going to be used. It is seen that when the PTMG molecular weight are decreased the peak corresponding to the  $\tan\delta$  value is more displace to the right. Reducing the PTMG molecular weight, the amount of heat to see the  $T_g$  is higher as the polymer is going to be stiffer, since the hydrogen bonding between the hard-segments provide an increased rigidity.<sup>56</sup> Samples

synthesised with PTMG 250/IPDI/CO N= 5 and N= 6 have shown higher  $T_g$  results among all the samples (*Attachment Table 35*).

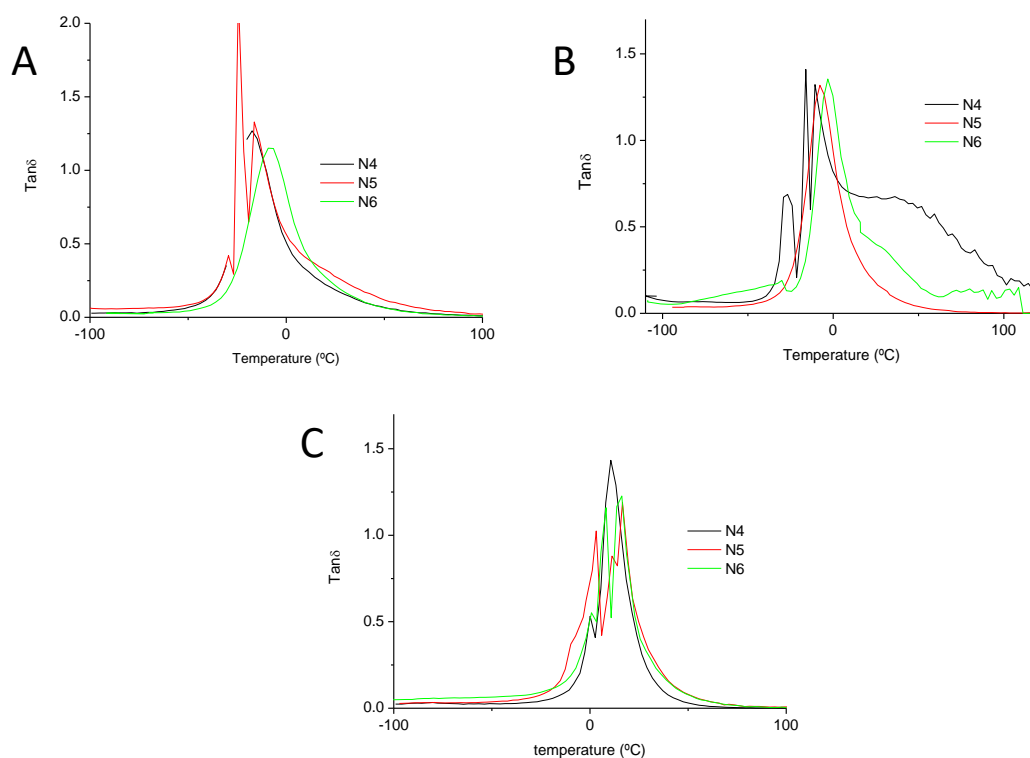


**Figure 30.**  $Tan\delta$  values for PTMG/IPDI/CO samples at PTMG 1000 (A) PTMG 650 (B) and PTMG 250 (C).

Last characterization technique used has been thermomechanical analysis. TMA has been used to check if synthesised PUs are able to reproduce SME. To check this out, the polymers have been deformed, fixed and recovered their shape. Following, each parameter is going to be studied (*Attachment Table 4S*). Starting with the deformation, there has not been found a linear relation between the N value and the  $R_d\%$ . *Figure 31 A* sample N= 5 exhibit a higher level of deformation rather than N= 4, also this effect can be seen in *Figure 31 B* and *Figure 31 C*. That effect was not expected, since as the N value is increased also the  $H_S\%$  does, meaning that samples are stiffer putting up resistance for being deformed as the chain movement is more restricted.<sup>27</sup> Continuing with  $R_f$  values, all PUs have shown very similar percentages, meaning that their original shape has been changed into a temporary one and they are able to maintain their new shape. Last

parameter examined is  $R_r\%$ . There has not been found any relation between the increase of the N value and recovery, however obtained percentage assure that samples are able to recover their initial shape been able to perform the SME. <sup>27</sup>

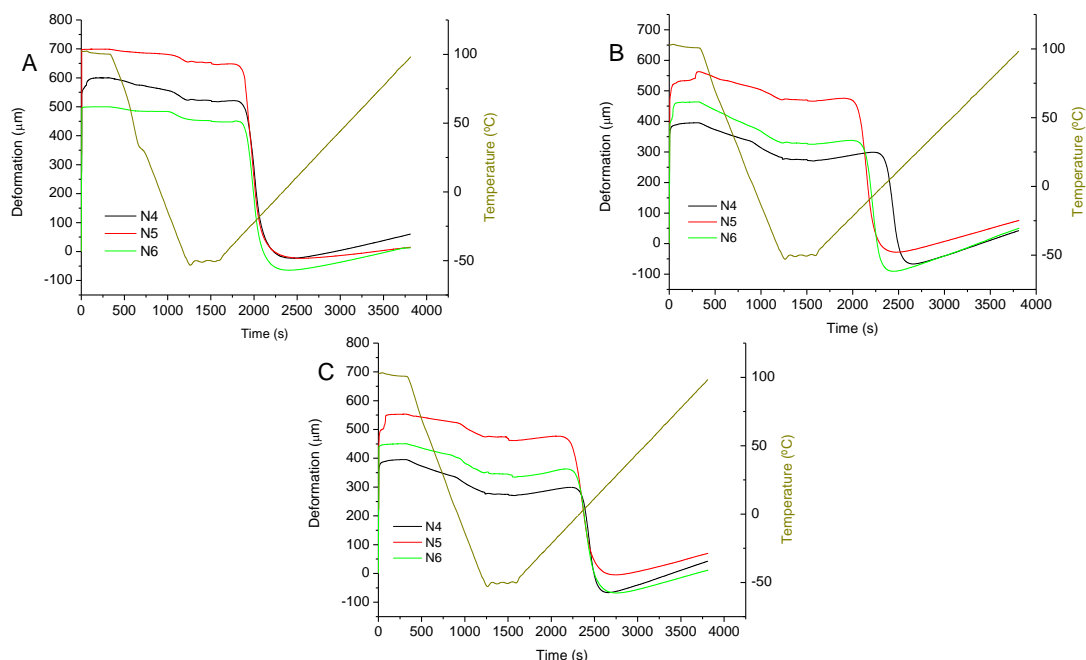


**Figure 31.** Cyclic process of SME effect exhibiting in Y axe force, deformation and temperature during a period of time Y axe for sample PTMG/IPDI/CO at PTMG 1000 (A), PTMG 650 (B) and PTMG 250 (C).

#### 4.2 SAMPLE CHARACTERIZATION AT NCO/OH= 1.05 AND 1.1 RATIOS

After analysis all the data corresponding to NCO/OH= 1, it was decided to upward the stoichiometry to NCO/OH= 1.05 and 1.1 ratios for polymers exhibiting best physical-chemical properties which were PTMG 250/IPDI/CO N= 5 and N= 6. The aim is to get higher HS% getting a stiffer polymer, which should show better mechanical and thermal properties.

After preparing the samples at higher ratios, the characterization of them was done. TGA analysis did not show any improvement comparing with samples at stoichiometry NCO/OH= 1 ratio. In *Figure 32* it is observed that  $T_i$  and experimental HS% values have not been improvement since  $T_i$  is almost the same, and the HS% have not increased getting a value close to theoretical (*Attachment Table 2S*). In these samples, from the



derivative also a third peak is seen, furthermore in NCO/OH = 1.05 for N= 6 the peak seems to be more accentuated.

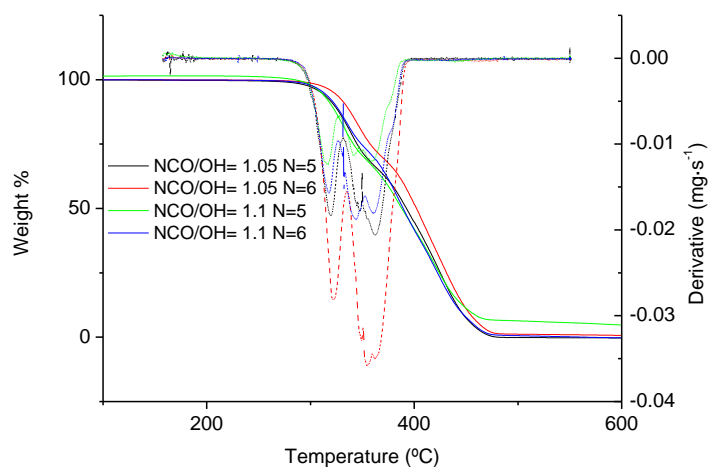


**Figure 32.** N= 5 and N= 6 samples with PTMG 250/IPDI/CO at NCO/OH= 1.05 and 1.1 in continue lines  $T_i$  and HS-SS% while in dash lines the derivative.

Next characterization technique has been DMA showing in *Figure 33*. Samples at stoichiometry NCO/OH= 1.05 ratio, show higher  $T_g$  value for N= 5 than N= 6, same happens in NCO/OH= 1.1 ratio. Comparing samples at same N value but at different ratios, samples at N= 5 exhibit more right  $Tan\delta$  displaced for 1.05 ratio than 1.1, same tendency is observed at N= 6. This tendency was not expected, since increasing the NCO/OH ratio also does the HS%. That means, that the sample should need higher temperatures to become rubbery showing a higher  $T_g$  value at NCO/OH= 1.1 ratio than in NCO/OH= 1.05 and at N= 6 than N= 5 (*Attachment Table 3S*). Comparing these samples with NCO/OH= 1 ratio, increasing the stoichiometry ratio there has not been an improve in  $T_g$  value.

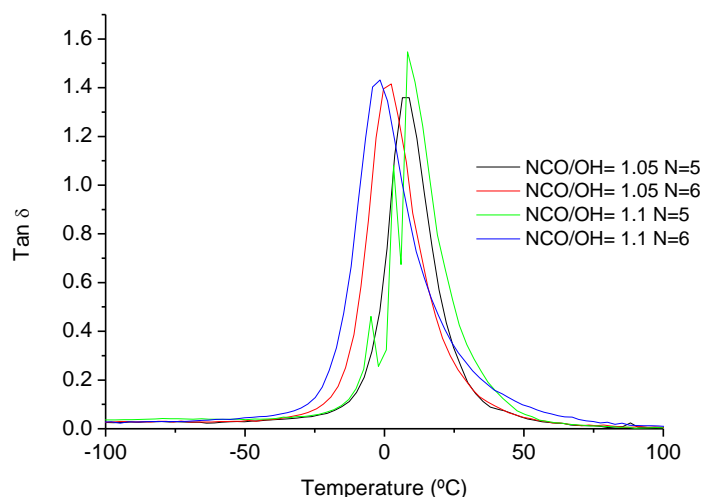


**Figure 33.** *Tan δ* from DMA technique values for samples PTMG 250/IPDI/CO at NCO/OH = 1.05 and 1.1 for N=5 and N=6.

Continuing with TMA (Figure 34) deformation, fixing and recovery values have been calculated showing them in Attachment Table 45. Samples at NCO/OH= 1.05 and NCO/OH= 1.1 exhibit similar deformation, fixing and recovery values comparing with NCO/OH= 1 ratio. With an increase in stoichiometry ratio TMA results were thought to be lower, since with more HS the polymer has less ability to deform. Yet, comparing the data obtained has been very similar for samples at three different stoichiometry ratios.

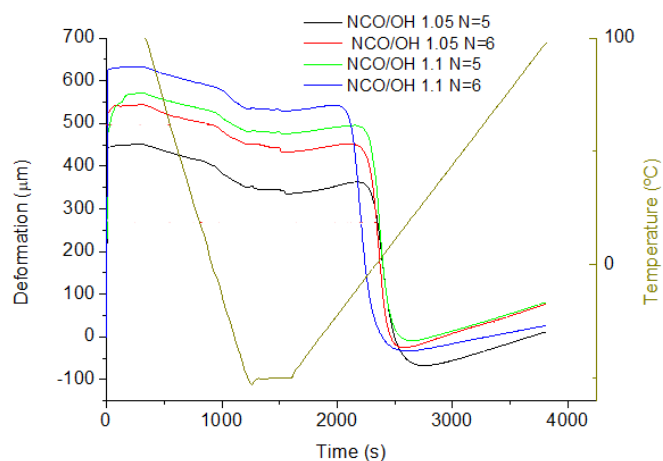


**Figure 34.** TMA analysis of samples PTMG 250/IPDI/CO NCO/OH= 1.05 and 1.1 at N=5 and N=6.

### 4.3 CYTOTOXIC ANALYSIS

Since a bio-renewable source has been used, results part will conclude showing the results from the cytotoxic analysis. Biocompatibility essays are studied with cell poliproliferation (amount of living cells in a sample) using method explained in 3.3.6 Chapter. Cell poliproliferation has been measured in *control%*, as well, the *control%* is an indicative of 100% of cell poliproliferation meaning that the material is utterly compatible. Sample biocompatibility is determine after 48 and 72 hours, comparing the percentage of cell poliproliferation with the control percentage considering biocompatible when the percentage of living cells is 50% or above.

All synthesised PUs contained CO instead of BD or other CE. The reason of choosing CO has been that previously was already checked cell proliferation percentage of PUs containing CO, BD and a mix of them (BD+CO).<sup>42</sup> Results showed that samples containing BD and a mix of CO+BD were not biocompatible as the percentage of cell proliferation was below 50%. Yet, those samples having just CO showed 60% of proliferation after 48 hours and 65% after 72 hours. Therefore, in order to get biocompatible SMPUs all the synthesis have been done using only CO as chain extender.

Biocompatibility effect has been analysed using PTMG at 1000, 650 and 250 g·mol<sup>-1</sup> maintaining the same isocyanate (IPDI), chain extender (CO) and stoichiometry (N= 5) in all the SMPUs. Reducing the PTMG molecular weight (*Figure 35*), it is observed that the percentage of cell proliferation increases in measures after 48 and 72 hours.

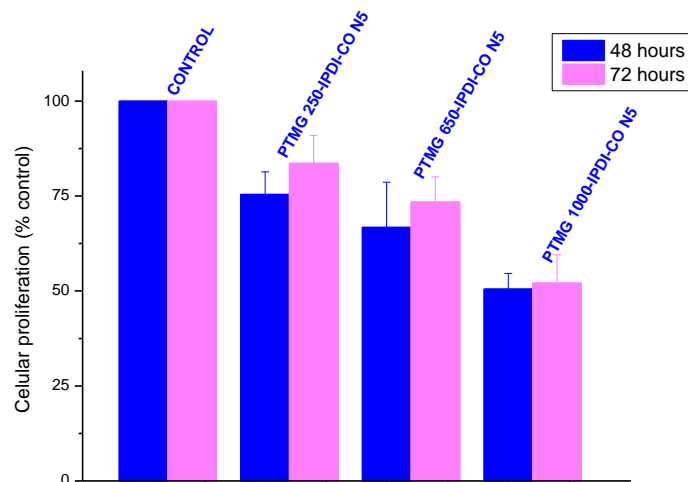


**Figure 35.** Percentage of cell proliferation reducing the PTMG molecular weight 1000-650-250 g·mol<sup>-1</sup> at N= 5 for PTMG /IPDI/CO samples.

## 5. CONCLUSIONS

In this study, castor oil based SMPUs have been synthesised using different PTMGs mass (1000, 650 and 250 g·mol<sup>-1</sup>) and aliphatic diisocyanate, IPDI. There have been applied different characterization techniques, such as ATR-FTIR, TGA, DMA, DSC and TMA in order to determine the physical-chemical properties, and also a cytotoxic evaluation for biocompatibility effect.

Using ATR-FTIR it has been assured that the SMPUs synthesis was complete, although in some samples it has been seen that not all the isocyanate has reacted. That is an important issue, since having free –NCO will lead to get less HS% and also less biocompatibility. TGA analysis has shown similar T<sub>i</sub> values for all synthesised SMPUs. Also with the first derivative, at 300°C peak corresponding to hard segment and at 400°C peak of SS have been determined, however, in some samples a third peak could be seen. In order to clarify that peak TGA-IR technique has been used, however, only bands belonging to small hydrocarbon chain molecules, N-H and carbonyl stretching bands were in this way associated to urethane group characteristic vibrations.

DSC and DMA results were in agreement. Increasing the N values in samples containing the same PTMG molecular weight, the T<sub>g</sub> value increases. Also the T<sub>g</sub> increases when

molecular weight of PTMG is reduced from  $1000 \text{ g}\cdot\text{mol}^{-1}$  to  $250 \text{ g}\cdot\text{mol}^{-1}$ . These effects are related with the HS% in both cases. In the first case, increasing the percentage of this segment the chain mobility is more restricted as there are more H-bonds between the HS requiring more thermal energy to produce the transition to amorphous state, thus, increasing the  $T_g$  value in DSC analysis. With DMA analysis, a higher need of temperature was needed to see a displacement in  $\text{Tan}\delta$ . As the polymer is stiffer can store energy elastically upon deformation requiring higher need of temperature to see the  $T_g$  values.

TMA results showed that all SMPUs are able to perform the SME since when they are reheated, they could recover the initial shape. There is not a linear relation between increasing the N value and deformation percentage and fixing values have been very similar in all samples.

Among all samples, PTMG 250/IPDI/CO N= 5 and N= 6 have exhibited best physical-chemical properties. Due to that, the stoichiometry have been increased from NCO/OH= 1 to 1.05 and 1.1 ratios. Comparing NCO/OH= 1 with samples with new ratios, TGA and TMA characterization techniques have shown similar results while DMA and DSC have exhibited lower  $T_g$  values.

Biocompatibility evaluation has shown that reducing the PTMG molecular weight cell proliferation percentage increases getting results of 75% and 80% after 48 and 72 hours for PTMG 250/IPDI/CO. CO and IPDI seems to be a promising alternative to get biocompatible SMPUs, since cell proliferation percentage increases comparing with samples containing BD or a mix of BD+CO.

## **6. FUTURE WORK**

PU's research is going to be continue with the synthesis of PTMG/IPDI/CO in order to get biocompatible and non-toxic polymers. The investigation will be focus on processing fibres and characterizing them in order to produce textiles which will also be characterized to ensure good physical-chemical properties. Also, thermogravimetric

analysis - mass spectrometry (TGA-MS) technique have been proposed in order to characterise the third peak that appears in some samples.

## **7. ACKNOWLEDGMENTS**

I would like to thank LabQuiMac for letting me perform the final degree project inside their group. Special thanks to my director Dr. Antonio Veloso for guiding me during these months and also to Dr. Jose Manuel Laza for been there every time I need help in the laboratory and teaching me how to use all the equipment that appear in this work. Last, I would like to thank Basque centre for Biophysic for doing biocompatibility essays and Tekniker for producing the fibres.

## **8. REFERENCES**

- (1) Sun, L.; Huang, W. M. Mechanisms of the Multi-Shape Memory Effect and Temperature Memory Effect in Shape Memory Polymers. *Soft Matter* **2010**, *6*, 4403–4406.
- (2) Lendlein, A., M. Schmidt, A., and L. .AB-Polymer Networks Based on Oligo( $\epsilon$ -Caprolactone) Segments Showing Shape-Memory Properties. *PNAS* **2001**, *98*, 842–847.
- (3) Peponi, L.; Navarro-baena, I.; Sonseca, A.; Gimenez, E.; Marcos-fernandez, A.; Kenny, J. M. Synthesis and Characterization of PCL – PLLA Polyurethane with Shape Memory Behavior. *Eur. Polym. J.* **2013**, *49*, 893–903.
- (4) García, N. Development and Applications of Semicrystalline Polymers : From Shape Memory To Self-Healing Materials. Ph.D. Thesis, universidad del pais vasco, Leioa, **2017**.
- (5) Ge, Q.; Luo, X.; Iversen, C. B.; Mather, P. T.; Dunn, M. L.; Qi, H. J. Mechanisms of Triple-Shape Polymeric Composites Due to Dual Thermal Transitions. *Soft Matter* **2013**, *9*, 2212–2223.
- (6) Ming Tian, Weisheng Gao, Jing Hu, Xiaowei Xu, Nanying Ning, Bing Yu, and L. Z. Multidirectional Triple-Shape-Memory Polymer by Tunable Cross-Linking and Crystallization. *ACS Appl. Mater. Interfaces* **2020**, *12*, 6426–6435.
- (7) Lendlein, A.; Kelch, S. Shape-Memory Effect From Permanent Shape. *Angew. Chem. Int. Ed. Engl.* **2002**, *41*, 2034–2057.
- (8) Barriando, L. H.; Jovancic, P. Formulación, Extrusión, Caracterización y Procesado Por Impresión 3D de Un Poliuretano Con Memora de Forma Para La Facribación de

Tejidos Funcionales Con Memoria de Forma. Ph.D. Thesis, universidad politecnica de Barcelona, Barcelona, **2017**.

(9) Akindoyo, J. O.; Beg, M. D. H.; Ghazali, S.; Islam, M. R.; Jeyaratnam, N.; Yuvaraj, A. R. Polyurethane Types, Synthesis and Applications-a Review. *RSC Adv.* **2016**, *6*, 114453–114482.

(10) Meng, H.; Li, G. A Review of Stimuli-Responsive Shape Memory Polymer Composites. *Polymer (Guildf)*. **2013**, *54*, 2199–2221.

(11) Cao, F.; Jana, S. C. Nanoclay-Tethered Shape Memory Polyurethane Nanocomposites. *Polymer (Guildf)*. **2007**, *48*, 3790–3800.

(12) More, A. S.; Lebarbé, T.; Maisonneuve, L.; Gadenne, B.; Alfos, C.; Cramail, H. Novel Fatty Acid Based Di-Isocyanates towards the Synthesis of Thermoplastic Polyurethanes. *Eur. Polym. J.* **2013**, *49*, 823–833.

(13) U.S. Energy Information Administration  
<https://www.eia.gov/todayinenergy/detail.php>.(accessed 9/12/2020).

(14) G. N. Chen and K. N. Chen. Self-Curing Behaviors of Single Pack Aqueous-Based Polyurethane System. *J. Appl. Polym. Sci.* **1997**, *63*, 1609–1623.

(15) Hu, J.; Chen, S. A Review of Actively Moving Polymers in Textile Applications. *J. Mater. Chem.* **2010**, *20*, 3346–3355.

(16) Mirabedini, A.; Foroughi, J.; Wallace, G. G. Developments in Conducting Polymer Fibres: From Established Spinning Methods toward Advanced Applications. *RSC Adv.* **2016**, *6*, 44687–44716.

(17) Horrocks, A. R., & Anand, S. Handbook of Technical Textiles. Elsevier. In *Handbook of technical textiles.*; **2000**;508–509.

(18) Sáenz-Pérez, M.; Lizundia, E.; Laza, J. M.; García-Barrasa, J.; Vilas, J. L.; León, L. M. Methylene Diphenyl Diisocyanate (MDI) and Toluene Diisocyanate (TDI) Based Polyurethanes: Thermal, Shape-Memory and Mechanical Behavior.Ph.D Thesis, universidad del pais vasco, Leioa, **2016**.

(19) Textile information <http://textileinformation.weebly.com/fabric.html> (accessed 9/12/2020).

(20) Textile school <https://www.textileschool.com/169/warp-knitting/> (accessed Dec 9/12/ 2020).

(21) Song, Z.; Xiao, H.; Zhao, Y. Hydrophobic-Modified Nano-Cellulose Fiber/PLA Biodegradable Composites for Lowering Water Vapor Transmission Rate (WVTR) of Paper. *Carbohydr. Polym.* **2014**, *111*, 442–448.

- (22) Sardon H, González A, Fernández-Berridi MJ, I. L. Oxygen Barrier Properties of Waterborne Polyurethane/Silica Hybrids. *J Macromol Sci Part B* **2015**, *54*, 711–721.
- (23) Sánchez Martín, J. R. Los Tejidos Inteligentes y El Desarrollo Tecnológico de La Industria Textil. *Técnica Ind.* **2007**, *268*, 38–45.
- (24) Mitsubishi Corporation Fashion CO., Ltd <https://www.mcf.co.jp/en/service/diaseries/diaplex.html> (accessed 25/12/2020).
- (25) Ionescu, M. Chemistry and Technology of Polyols for Polyurethanes. In *Chemistry and technology of polyols for polyurethanes*. iSmithers Rapra Publishing; **2005**; 23–25.
- (26) Aís, F. A. Síntesis y Caracterización de Poliuretanos Termoplásticos Que Contienen Resinas de Colofonia y Su Aplicación. Ph.D. Thesis, universidad de Alicante, Alicante, **2000**.
- (27) Klinedinst, D. B.; Yilgör, I.; Yilgör, E.; Zhang, M.; Wilkes, G. L. The Effect of Varying Soft and Hard Segment Length on the Structure-Property Relationships of Segmented Polyurethanes Based on a Linear Symmetric Diisocyanate, 1,4-Butanediol and PTMO Soft Segments. *Polymer (Guildf)*. **2012**, *53*, 5358–5366.
- (28) Autor, M.; Mestre, G.; Convocat, G. Síntesis y Caracterización de Poliuretanos Derivados de La Glucosa Para Aplicaciones Como Recubrimientos Sostenibles. Ph.D Thesis, universidad politecnica de cataluña, Barcelona, **2017**.
- (29) Bocchio, J. A.; Quagliano, J. C. Influencia Del Contenido de Nanoarcilla En La Cinética de Curado de Un Poliuretano Basado En Pbht. *Revista iberoamericana de bocchio y Quagiano* **2017**, *18*, 1–8.
- (30) Ylgor, E.; Ylgor, I.; Yurtsever, E. Hydrogen Bonding and Polyurethane Morphology. I. Quantum Mechanical Calculations of Hydrogen Bond Energies and Vibrational Spectroscopy of Model Compounds. *Polymer (Guildf)*. **2002**, *43*, 6551–6559.
- (31) Carbonell-Blasco, P. Adhesivos de Poliuretano Termoplásticos Potencialmente Biodegradables Obtenidos Con Derivados de Productos Naturales. Ph.D. Thesis, universidad de Alicante, Alicante, **2013**.
- (32) de Castro, P. F. Síntesis y Caracterización de Poliuretanos Termoplásticos Basados En Policarbonato Dioles. Relación Estructura/Propiedades. Ph.D. Thesis, universidad de Valencia, Valencia, **2012**.
- (33) Mitsubishi chemicals [https://www.m-chemical.co.jp/en/products/departments/mcc/c4/product/1201008\\_7922.html](https://www.m-chemical.co.jp/en/products/departments/mcc/c4/product/1201008_7922.html) (accessed 15/09/2020).



- (34) Barbadillo Jove, F. Estudio Cinético de Degradación Térmica de Poliuretanos Mediante Análisis Termogravimétrico (TGA). Ph.D. Thesis, universidad de Acoruña, Acoruña, **2015**.
- (35) Uscategui, Y. L., Díaz, L. E., & Valero, M. F. Aplicaciones Biomédicas de Poliuretanos. *Quim. Nova* **2018**, *41*, 434–445.
- (36) Sánchez-Adusar, M. . Síntesis y Caracterización de Poliuretanos Termoplásticos: Aplicación a La Formulacion de Adhesivos. Ph.D. Thesis, universidad de Alicante, Alicante, **1996**.
- (37) Gurunathan, T.; Mohanty, S.; Nayak, S. K. Isocyanate Terminated Castor Oil-Based Polyurethane Prepolymer: Synthesis and Characterization. *Prog. Org. Coatings* **2015**, *80*, 39–48.
- (38) Elicriso revista sobre el entorno y naturaleza [https://www.elicriso.it/es/plantas medicinales](https://www.elicriso.it/es/plantas-medicinales) (accessed 4/09/2020).
- (39) Sokolowski, W.; Metcalfe, A.; Hayashi, S.; Yahia, L.; Raymond, J. Medical Applications of Shape Memory Polymers. *Biomed. Mater.* **2007**, *2*, S23.
- (40) Ratna, D.; Karger-Kocsis, J. Recent Advances in Shape Memory Polymers and Composites: A Review. *J. Mater. Sci.* **2008**, *43*, 254–269.
- (41) Sonas home health care <https://www.sonashomehealth.com/what-is-deep-vein-thrombosis/> (accessed 8/12/2020).
- (42) Taguado, M. Síntesis y Caracterización de Propiedades Mecánicas de Poliuretanos Biocompatible. TFG, universidad del pais vasco , Leioa, **2019**.
- (43) Sierra, S. Forma-Memoria Duten Poliuretano Biobateragarrien Sintesia Eta Propietate Mekanikoen Karakterizazioa. TFG, universidad del pais vasco, Leioa, **2019**.
- (44) Wang, Z.; Yu, L.; Ding, M.; Tan, H.; Li, J.; Fu, Q. Preparation and Rapid Degradation of Nontoxic Biodegradable Polyurethanes Based on Poly(Lactic Acid)-Poly(Ethylene Glycol)-Poly(Lactic Acid) and L-Lysine Diisocyanate. *Polym. Chem.* **2011**, *2*, 601–607.
- (45) Prime, R. B., Bair, H. E., Vyazovkin, S., Gallagher, P. K., & Riga, A. Thermogravimetric Analysis (TGA). Thermal Analysis of Polymers: Fundamentals and Applications. In *Thermogravimetric analysis (TGA). Thermal analysis of polymers: Fundamentals and applications*; **2009**;241–317.
- (46) Mettler Toledo.[www.wvu.edu/TA Instruments QDSC Differential Scanning Calorimeter Getting Started.pdf](http://www.wvu.edu/TA_Instruments_QDSC_Differential_Scanning_Calorimeter_Getting_Started.pdf) (accessed 15/10/2020).
- (47) Mettler Toledo  
[https://www.mt.com/es/es/home/products/Laboratory\\_Analytics\\_Browse/TA\\_Family\\_Browse/DSC.html](https://www.mt.com/es/es/home/products/Laboratory_Analytics_Browse/TA_Family_Browse/DSC.html) (accessed 15/10/2020).

- (48) Mettler Toledo DMA analysis  
[https://www.mt.com/int/en/home/products/Laboratory\\_Analytics\\_Browse/TA\\_Family\\_Browse/DMA.html](https://www.mt.com/int/en/home/products/Laboratory_Analytics_Browse/TA_Family_Browse/DMA.html) (accessed 15/10/2020).
- (49) Rimdusit, S., & Ishida, H. Synergism and Multiple Mechanical Relaxations Observed in Ternary Systems Based on Benzoxazine, Epoxy, and Phenolic Resins. *J. Polym. Sci. Part B Polym. Phys.* **2000**, *38*, 1687–1698.
- (50) Vinardell Martínez-Hidalgo, M. P. Alternativas a La Experimentación Animal En Toxicología: Situación Actual. *Acta Bioeth.* **2007**, *13*, 41–52.
- (51) Gallegos-Hernandez, G. F. *Ensayos Colorimétricos Para La Detección de Citotoxicidad; Vidsupra vison cientidica*, **2018**, *10*, 1-4.
- (52) Uscategui, Y. L.; Díaz, L. E.; Valero, M. F. Actividad Antibacteriana, Degradación Hidrolítica y Microbiana y Citotoxicidad in Vitro de Poliuretanos Sintetizados Con Polioles Derivados Del Aceite de Higuera. *Quím. Nov.* **2017**, *40*, 131-137.
- (53) Corcuera, M. A.; Rueda, L.; Fernandez D’Arlas, B.; Arbelaz, A.; Marieta, C.; Mondragon, I.; Eceiza, A. Microstructure and Properties of Polyurethanes Derived from Castor Oil. *Polym. Degrad. Stab.* **2010**, *95*, 2175–2184.
- (54) Cervantes-Uc, J. M.; Espinosa, J. I. M.; Cauch-Rodríguez, J. V.; Ávila-Ortega, A.; Vázquez-Torres, H.; Marcos-Fernández, A.; Román, J. S. TGA/FTIR Studies of Segmented Aliphatic Polyurethanes and Their Nanocomposites Prepared with Commercial Montmorillonites. *Polym. Degrad. Stab.* **2009**, *94*, 1666–1677.
- (55) Takahashi, T., Hayashi, N., & Hayashi, S. Structure and Properties of Shape-memory Polyurethane Block Copolymers. *J. Appl. Polym. Sci.* **1996**, *60*, 1061–1069.
- (56) Mondal, S.; Hu, J. L. Water Vapor Permeability of Cotton Fabrics Coated with Shape Memory Polyurethane. *Carbohydr. Polym.* **2007**, *67*, 282–287.

## **9. ATTACHMENTS**

### **9.1 ACRONYMS**

ATR-FTIR: Attenuated total reflection - Fourier transform infrared spectroscopy

BD: 1, 4 butanediol

CE: Chain extender

CO: Castor oil

DMA: Dynamic mechanical analysis

DSC: Differential scanning calorimetry

DSME: Dual-shape memory effect

$E^*$ : Complex Young module

$E'$ : Storage module

$E''$ : Loss factor

FPU: Flexible Polyurethane

H-bond: Hydrogen bond

HDI: Hexamethylene diisocyanate

HS: Hard segment

IPDI: Isophorone diisocyanate

MDI: diphenilmethane-4,4-diisocyanate

N: Stoichiometry relation

PO<sub>2</sub>: Permeability Oxygen Measurements

PTMG: Poly (tetramethylene ether) glycol

PU: Polyurethane

PUD: Polyurethane dispersion

PUI: Polyurethane ionomer

R<sub>d</sub>: Deformation

R<sub>f</sub>: Fixing

R<sub>r</sub>: Recovery

SME: Shape-memory effect

SMF: Shape-memory fibres

SMM: Shape-memory materials

SMP: Shape-memory polymer

SMPU: Shape-memory polyurethane

SRM: Stimulus responsive materials

SS: Soft segment

Tan $\delta$ : Loss factor or loss tangent

T<sub>D</sub>: Derivative maximum degradation temperature

T<sub>D1</sub>: First maximum temperature degradation peak

T<sub>D2</sub>: Second maximum temperature degradation peak

TDI: Toluene-2,4-diisocyanate

T<sub>g</sub>: Glass transition temperature or vitreous transition state

TGA: Thermogravimetry analysis

TGA-IR: Thermogravimetric analysis - infrared spectroscopy

TGA-MS: Thermogravimetric analysis-mass spectrometry

T<sub>i</sub>: Initial thermal stability temperature

TMA: Thermomechanical analysis

TPU: Thermoplastic polyurethane

TSME: Triple-shape memory effect

T<sub>Trans</sub>: Transition temperature

WPU: Waterborne polyurethane

WPUD: Waterborne polyurethane dispersion

WVTR: Water Vapour Transmission rate

## 9.2 TABLES

**Table 1S.** *Polyurethane bands assignment*

<b>Band assignment</b>	<b>Wavenumber (cm<sup>-1</sup>)</b>
V NH	3320
V C=O	1700
V C-O-C	1100
V N=C=O	2270
$\delta$ C-N	1530

**Table 2S.** Results of  $T_i$ ,  $T_D$ , experimental HS% and theoretical HS% got from TGA analysis

POLYURETHANE	$\frac{NCO}{OH}$	N	TGA				
			$T_i(^{\circ}C)$	$T_{D1}(^{\circ}C)$	$T_{D2}(^{\circ}C)$	Experimental %HS	Theoretical %HS
PTMG 1000/IPDI/CO	1	4	290.6	330.5	407.8	56.2	82.8
	1	5	294.8	335.9	414.2	59.7	85.7
	1	6	282.0	332.9	413.8	56.3	87.7
PTMG 650/IPDI/CO	1	4	301.0	340.0	422.0	29.6	88.1
	1	5	293.0	333.3	412.6	30.8	90.2
	1	6	299.9	333.2	418.2	39.1	91.6
PTMG 250/IPDI/CO	1	4	285.8	321.1	365.4	47.8	95.0
	1	5	301.0	340.0	423.0	50.4	96.0
	1	6	290.6	327.5	375.6	52.6	96.6
PTMG 250/IPDI/CO	1.05	5	279.2	337.2	427.1	44.6	97.8
	1.05	6	296.0	343.4	416.7	47.3	97.0
	1.1	5	294.6	330.2	421.2	41.6	96.0
	1.1	6	287.9	333.4	424.0	48.9	96.6

**Table 3S.** Results for  $T_g$  value got from DSC and  $Tan\delta$  of DMA

POLYURETHANE	$\frac{NCO}{OH}$	N	DSC		DMA
			$T_g$ On set (°C)	$T_g$ End set(°C)	$Tan\delta$ (°C)
PTMG 1000/IPDI/CO	1	4	-39.0	-24.6	-17.4
	1	5	-36.7	-26.2	-16.3
	1	6	-38.7	-20.8	-6.5
PTMG 650/IPDI/CO	1	4	-41.5	-27.9	-10.6
	1	5	-30.8	-14.3	-7.8
	1	6	-28.8	-13.8	-3.1
PTMG 250/IPDI/CO	1	4	-11.2	0.8	10.6
	1	5	-17.9	-1.1	16.5
	1	6	-15.2	2.1	16.2
PTMG 250/IPDI/CO	1.05	5	-	-	9.9
	1.05	6	-	-	2.4
	1.1	5	13.8	0.1	8.2
	1.1	6	29.6	-14.2	-1.5



**Table 4S.** Percentage of  $R_d$ ,  $R_f$  and  $R_r$  calculated from TMA technique

POLYURETHANE	$\frac{NCO}{OH}$	N	TMA		
			Deformation% ( $R_d$ )	Fixing% ( $R_f$ )	Recovery% ( $R_r$ )
PTMG 1000/IPDI/CO	1	4	11.2	93.0	89.6
	1	5	13.9	92.5	98.1
	1	6	9.9	90.9	97.4
PTMG 650/IPDI/CO	1	4	9.2	93.0	89.6
	1	5	11.0	82.3	88.3
	1	6	10.5	52.7	93.0
PTMG 250/IPDI/CO	1	4	7.7	77.6	89.7
	1	5	10.9	86.8	87.6
	1	6	8.8	81.5	98.1
PTMG 250/IPDI/CO	1.05	5	10.0	84.3	85.8
	1.05	6	10.5	82.9	85.5
	1.1	5	10.7	93.1	85.4
	1.1	6	12.4	86.2	95.8

**Table 5S.** Percentage of cell proliferation after 48 and 72 hours.

POLYURETHANE	N	Cell proliferation% after 48 Hours	Cell proliferation% after 72 Hours
PTMG 1000/IPDI/CO	5	50	52
PTMG 650/IPDI/CO	5	62	74
PTMG 250/IPDI/CO	5	75	80

